Bioorganic Chemistry 116 (2021) 105250

Contents lists available at ScienceDirect

Bioorganic Chemistry

journal homepage: www.elsevier.com/locate/bioorg

Synthesis and *in vitro* and *in silico* studies of 1*H*- and 2*H*-1,2,3-triazoles as antichagasic agents

Thais B. Silva [a], Kathya N.K. Ji [a], Fernanda Petzold Pauli [b], Raíssa M.S. Galvão [c,d], Ana F. M. Faria [e], Murilo L. Bello [c], Jackson A.L.C. Resende [f], Vinicius R. Campos [b], Luana da S. M. Forezi [b], Fernando de C. da Silva [b], Robson X. Faria [c,e,*], Vitor F. Ferreira [a,*]

[a] *Universidade Federal Fluminense, Departamento de Tecnologia Farmacêutica, Faculdade de Farmácia, Santa Rosa, CEP 24241-002 Niterói, RJ, Brazil*
[b] *Universidade Federal Fluminense, Instituto de Química, Departamento de Química Orgânica, Campus do Valonguinho, CEP 24020-150 Niterói, RJ, Brazil*
[c] *Fundação Oswaldo Cruz, Instituto Oswaldo Cruz, Laboratório de Toxoplasmose e outras Protozooses, Pavilhão Carlos Chagas, Manguinhos, CEP 21045-900 Rio de Janeiro, RJ, Brazil*
[d] *Universidade Federal Fluminense, Instituto de Biologia, Pós-graduação de Ciências e Biotecnologia, Campus do Valonguinho, CEP 24020-150 Niterói, RJ, Brazil*
[e] *Universidade Federal do Rio de Janeiro, Faculdade de Farmácia, Laboratório de Planejamento Farmacêutico e Simulação Computacional, CEP 21941-599 Rio de Janeiro, RJ, Brazil*
[f] *Universidade Federal de Mato Grosso, Instituto de Ciências Exatas e da Terra, Campus Universitário do Araguaia, CEP 78698-000 Pontal do Araguaia, MT, Brazil*

ARTICLE INFO

Keyword:
Dimroth rearrangement
Heterocycles
Azoles
Parasites
Trypanosoma cruzi
Epimastigote form

ABSTRACT

1,2,3-triazole heterocycles stand out in medicinal chemistry for having great structural diversity and bioactivities. In this study, two series of triazoles were synthesized. One was obtained by the 1,3-dipolar cycloaddition reaction between ethyl cyanoacetate and several phenyl azides forming 1*H*-1,2,3-triazoles and the other by rearrangement of Dimroth forming and 2*H*-1,2,3-triazoles. Both series were shown to be active against the *epimastigote* form of *Trypanosoma cruzi*. The 1,2,3-triazoles **16d** (S.I. between 100 and 200), **17d** and **16f** (S.I. > 200) were the most active compounds and capable of breaking the plasma membrane of trypomastigotes acting on CYP51 and inhibiting ergosterol synthesis. Candidate **16d** exhibited the best and most favorable profile when interacting with CYP51.

1. Introduction

Triazoles have been studied for over a century and continue to attract considerable attention due to its interesting bioactive properties. They are an important class of heterocyclic compounds and basic heterocyclic rings present in the various medicinal agents are 1,2,3-triazole and 1,2,4-triazole [1-3]. Fig. 1 shows some compounds containing the triazolic nucleus in its structure, commonly used as drugs for the treatment of various diseases [4-10]. They are resistant to metabolic degradation, stability to acid/basic hydrolysis, and reduction/oxidation conditions, a consequence of its aromatic character [1]. These heterocycles can have different isomeric structures. For example, 1,2,3-triazoles can occur mainly in two isomeric forms: 1H-1,2,3-triazole or 2H-1,2,3-triazole [11]. Because of the success of several members of the triazole family, many companies and research groups have shown interest in developing new methods of synthesis and biological evaluation of the potential uses of these compounds [12].

The most common synthetic method for the preparation of 1,2,3-triazoles is Huisgen cycloaddition [13,14] between azide and alkyne. The stepwise version of this cycloaddition with high regioselectivity for the 1,4-disubstituted isomer was developed by Sharpless and coworkers with the use of copper (I) as a catalyst [15-17] This method has become very popular and has been used in many syntheses of 1,2,3-triazoles for biological investigation [18-22].

Studies on the biological activity of 1,2,3-triazole analogs have shown that these compounds have diversified activities against microorganisms and various biological targets related to the important diseases. Specifically, we highlight the biological activity against T. cruzi, the etiologic agent that causes Chagas disease (Fig. 2) [23-30].

Due to the structural diversity of this scaffold, other methodologies [21] are required than Huisgen's concerted cycloaddition. Among these triazoles, we highlight the disubstituted 5-amino-1*H*-1,2,3-triazoles.

* Corresponding authors at: Fundação Oswaldo Cruz, Instituto Oswaldo Cruz, Laboratório de Toxoplasmose e outras Protozooses, Pavilhão Carlos Chagas, Manguinhos, CEP 21045-900 Rio de Janeiro, RJ, Brazil (R.X. Faria).
E-mail addresses: robson.xavier@gmail.com (R.X. Faria), vitorferreira@id.uff.br (V.F. Ferreira).

https://doi.org/10.1016/j.bioorg.2021.105250
Received 10 May 2021; Received in revised form 13 July 2021; Accepted 3 August 2021
Available online 11 August 2021

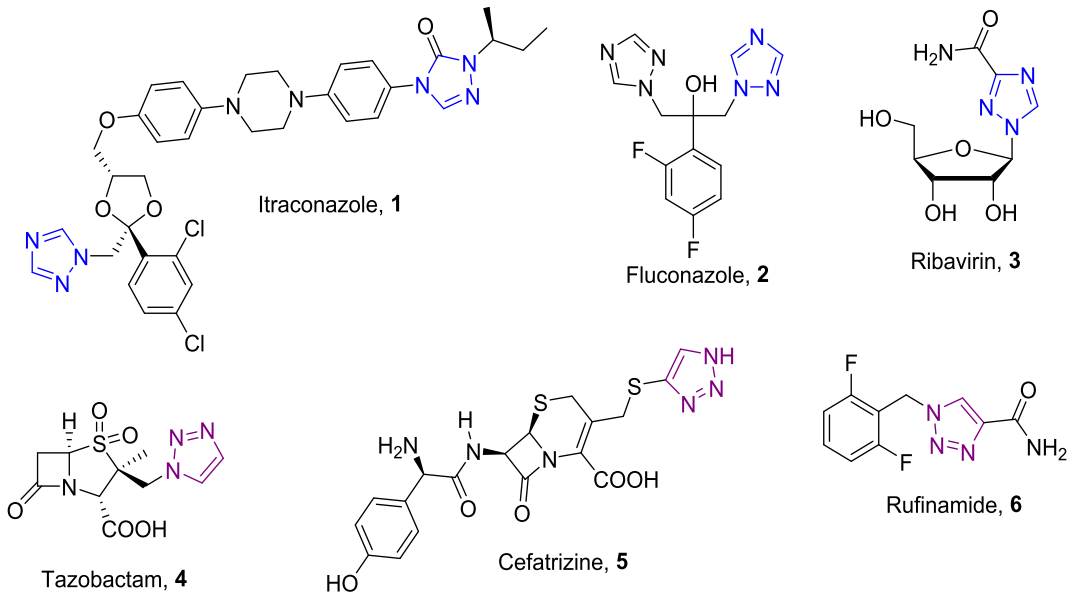

Fig. 1. Selected examples of drugs having the triazole moiety.

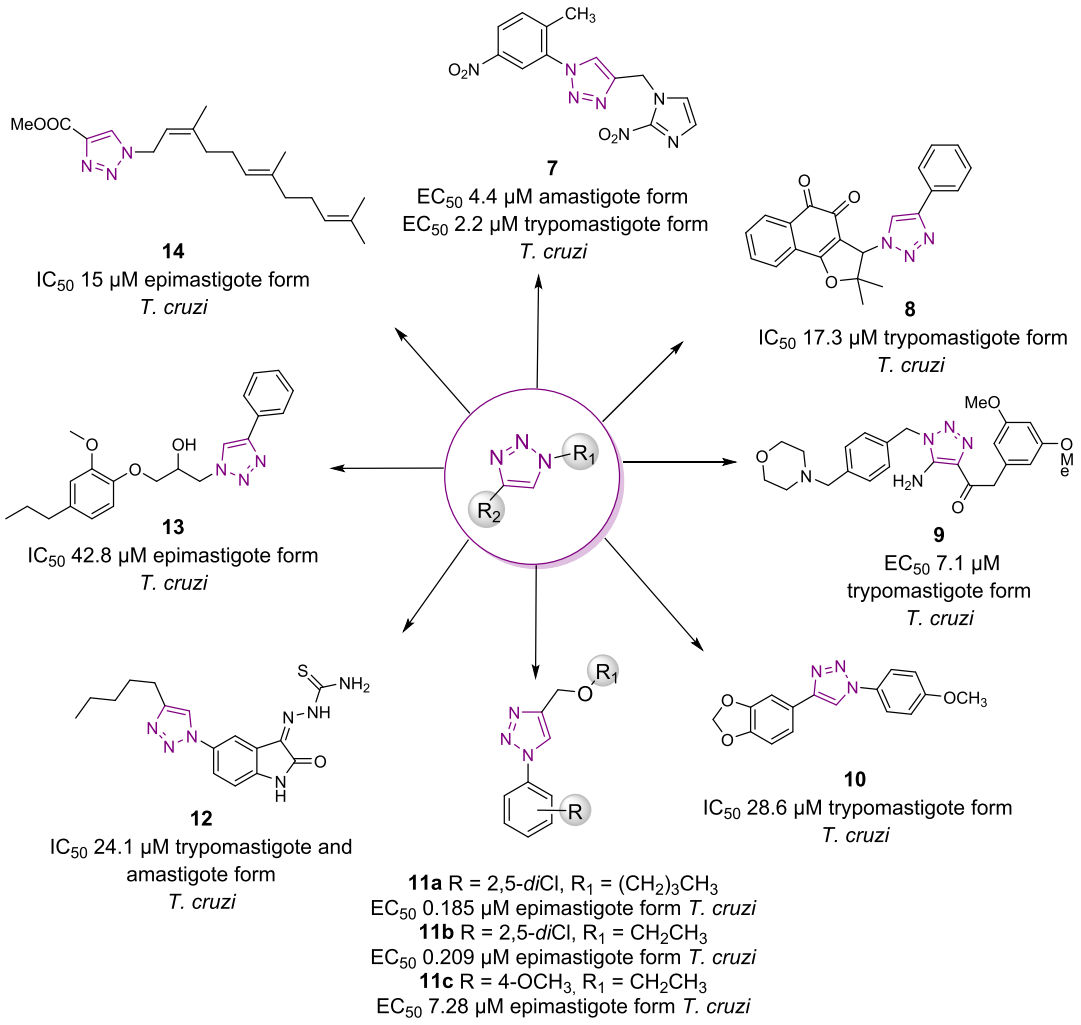

Fig. 2. 1*H*-1,2,3-Triazoles with trypanocidal activity.

These compounds can be obtained by the reaction between alkyl/aryl azides with cyanoacetate esters *via* enolate. It is important to note that Otto Dimroth discovered this cycloaddition in 1909 [31-33], and later expanded to other similar systems. However, the most important aspect of 5-amino-1*H*-triazoles is their ability to interconvert into an isomer with translocation of nitrogen atoms into the ring, forming 5-(arylamino)–2*H*-1,2,3-triazoles. This interconversion is known as Dimroth rearrangement (DR), which is much more comprehensive and useful in the preparation of new heterocycles [34].

In attempt to discover potential 1*H*- and 2*H*-triazoles with trypanocidal action, we herein describe the synthesis and trypanocidal evaluate of ethyl 5-amino-1-aryl-1*H*-1,2,3-triazole-4-carboxylates and ethyl 5-(arylamino)–2*H*-1,2,3-triazole-4-carboxylates.

2. Experimental section

2.1. Chemistry

The reagents, deuterated solvents and common solvents were bought from several commercial sources. Some of them were purified by usual techniques and some were used without further purification. Silica gel for flash column chromatography and silica gel thin layer chromatography plates (F254) were bought from Merck or Sigma Aldrich, respectively. The analyses with TLC plates were visualized by using UV light or revealed with aqueous solutions of ammonium sulfate. The reported yields of the triazoles refer to pure isolated compounds. Thermo scientific 9100 apparatus were used to obtain the melting points of the solids and are uncorrected. The spectrophotometer Perkin-Elmer model 1420 FT-IR was used to obtain the IR absorbance of the triazoles using KBr. The IR spectrophotometer was calibrated using polystyrene using the absorbance of 1601.8 cm^{-1}. ^{1}H and ^{13}C Nuclear Magnetic Resonance (NMR) were obtained in solution of deuterated solvents at room temperature using a Varian Mercury 300.00 MHz or Varian Mercury 500.00 MHz. The chemical shift of ^{1}H or ^{13}C are in units of δ (ppm) downfield from the deuterated solvent and the coupling constants J ^{1}H–^{1}H are reported in hertz unit, which refer to apparent peak multiplicities. High resolution mass spectra (HRMS) were recorded on a MICROMASS QTOF mass spectrometer (Waters).

X-ray diffraction data for cubebin was carried out with radiation MoKa (λ = 0.71073 Å) in Bruker D8 Venture diffractometer at room temperature. The data collection and cell refinement were performed using APEX3 (ref: Bruker APEX3, SAINT and SADABS Bruker AXS Inc., Madison, Wisconsin, USA). All structures were solved using Intrinsic Phasing and refinement package using Least Squares Methods with the SHELX programs [35] implemented in the Olex2 package. Non-hydrogen atoms were refined with anisotropic displacement parameters, and the hydrogen atoms were positioned geometrically using the riding model. Molecular graphics draw using Olex2 [36].

2.1.1. General procedure for exclusive obtaining ethyl 5-amino-1-phenyl-1H-triazole-4-carboxylates **16a-i**

A mixture of arylazide (**15a-i**, 0.01 mol) and ethyl cyanoacetate (0.01 mol) in 25 mL of dry ethanol containing 0.01 mol of sodium ethoxide was kept under stirring at room temperature in inert atmosphere during three hours. The reaction mixture was poured into 50 mL of ice water. The precipitate that formed was collected by filtration and washed with water to obtain **16a-i**.

Ethyl 5-amino-1-phenyl-1H-1,2,3-triazole-4-carboxylate (**16a**). 62% yield. m.p.: 130–131 °C (lit. [37] 130–131 °C); IR (KBr, cm^{-1}): 3422–3312, 2986, 1677, 1626, 1513, 1278–1259, 1109, 755–691; ^{1}H NMR (500.00 MHz, DMSO-d_6, TMS, δ ppm): 0.84 (t, 3H, *J* 7.1 Hz), 3.84 (q, 2H, *J* 7.1 Hz), 5.86 (s, 2H), 6.91 (t, 1H, *J* 4.4 Hz), 7.19–7.05 (m, 5H); HRMS (ESI) calc. for $C_{11}H_{12}N_4NaO_2$ 255.0858, found $[M+Na]^+$ 255.0844. Δ 5.5 ppm.

Ethyl 5-amino-1-(p-tolyl)-1H-1,2,3-triazole-4-carboxylate (**16b**). 65% yield. m.p.: 154–155 °C (lit. [37] 151–152 °C); IR (KBr, cm^{-1}): 3413–3282, 2978, 2926, 1686, 1626, 1519, 1263, 819–782; ^{1}H NMR (500.00 MHz, DMSO-d_6, TMS, δ ppm): 1.31 (t, 3H, *J* 7.1 Hz), 2.41 (s, 3H), 4.30 (q, 2H, *J* 7.1 Hz), 6.44 (s, 2H), 7.45–7.41 (m, 4H); HRMS (ESI) calc. for $C_{12}H_{14}N_4NaO_2$ 269.1014, found $[M+Na]^+$ 269.1015. Δ 0.4 ppm.

Ethyl 5-amino-1-(4-methoxyphenyl)1H-1,2,3-triazole-4-carboxylate (**16c**). 67% yield. m.p.: 140–141 °C (lit. [38] 138–139 °C); IR (KBr, cm^{-1}): 3433–3299, 1684, 1622, 1518, 1249, 833–782; ^{1}H NMR (500.00 MHz, DMSO-d_6, TMS, δ ppm): 1.32 (t, 3H, *J* 7.1 Hz), 3.85 (s, 3H), 4.31 (q, 2H, *J* 7.1 Hz), 6.24 (s, 2H), 7.14 (d, 2H, *J* 9.0 Hz), 7.46 (d, 2H, *J* 8.9 Hz); HRMS (ESI) calc. for $C_{13}H_{14}N_4O_3$ 263.1144, found $[M + H]^+$ 263.1136. Δ 3.0 ppm.

Ethyl 5-amino-1-(4-fluorophenyl)-1H-1,2,3-triazole-4-carboxylate (**16d**). 60% yield. m.p.: 130–131 °C (lit. [37] 128–129 °C); IR (KBr, cm^{-1}): 3451–3157, 2980, 2918, 1678, 1518, 1215, 836–781; ^{1}H NMR (500.00 MHz, DMSO-d_6, TMS, δ ppm): 1.33 (t, 3H, *J* 4.2 Hz), 4.2 (q, 2H, *J* 7.1 Hz), 6.47 (sl, 2H), 7.53 (t, 2H, *J* 9.1 Hz), 7.71 (dd, 2H, *J* 9.1 and 4.9 Hz); HRMS (ESI) calc. for $C_{11}H_{11}FN_4NaO_2$ 273.0764, found $[M+Na]^+$ 273.0761. Δ 1.1 ppm.

Ethyl 5-amino-1-(4-chloropheyl)-1H-1,2,3-triazole-4-carboxylate (**16e**). 60% yield. m.p.: 157–159 °C (lit. [37] 165–166 °C); IR (KBr, cm^{-1}): 3465–3293, 2982, 1716, 1629, 1511, 1132, 827–618; ^{1}H NMR (500.00 MHz, DMSO-d_6, TMS, δ ppm): 1.33 (t, 3H, *J* 7.1 Hz), 4.32 (q, 2H, *J* 7.1 Hz), 6.55 (s, 2H), 7.60 (d, 2H, *J* 8.9 Hz), 7.67 (d, 2H, *J* 8.8 Hz); HRMS (ESI) calc. for $C_{11}H_{11}ClN_4NaO_2$ 289.0468, found $[M+Na]^+$ 289.0461. Δ 2.4 ppm.

Ethyl 5-amino-1-(4-bromophenyll)-1H-1,2,3-triazole-4-carboxylate (**16f**). 93% yield. m.p.: 166–167 °C (lit. [39] 168–169 °C); IR (KBr, cm^{-1}): 3434–3166, 2983–2928, 1692, 1627, 1507, 1114, 820–700; ^{1}H NMR (500.00 MHz, DMSO-d_6, TMS, δ ppm): 1.32 (t, 3H, *J* 7.1 Hz), 4.32 (q, 2H, *J* 7.1 Hz), 6.46 (s, 2H), 7.53 (d, 2H, *J* 8.7 Hz), 7.80 (d, 2H, *J* 8.8 Hz); HRMS (ESI) calc. for $C_{11}H_{12}BrN_4NaO_2$ 332.9963, found $[M+Na]^+$ 332.9953. Δ 3.0 ppm.

Ethyl 5-amino-1-(2-chlorophenyl)-1H-1,2,3-triazole-4-carboxylate (**16g**). 56% yield. m.p.: 218–219 °C; ^{1}H NMR (300.00 MHz, DMSO-d_6, TMS, δ ppm): 1.32 (t, 3H, *J* 7.1 Hz), 4.32 (q, 2H, *J* 7.1 Hz), 6.52 (s, 2H), 7.55 (dt, *J* 1.9 and 7.0 Hz, 1H), 7.54–7.67 (m, 3H); HRMS (ESI) calc. for $C_{11}H_{11}ClN_4NaO_2$ 289.0468, found $C_{11}H_{11}ClN_4O_2$ 289.0470. Δ 0.7 ppm.

Ethyl 5-amino-1-(2,5-dichlorophenyl)-1H-1,2,3-triazole-4-carboxylate (**16h**). 65% yield. m.p.: 218–219 °C (lit. [38] 222–223 °C); IR (KBr, cm^{-1}): 3380, 2995, 1688, 1594, 779; ^{1}H NMR (300.00 MHz, DMSO-d_6, TMS, δ ppm): 1.33 (t, 3H, *J* 7.1 Hz), 4.32 (q, 2H, *J* 7.1 Hz), 6.58 (s, 2H), 7.72 (dd, 1H, *J* 8.7 and 2.5 Hz), 7.80 (d, 1H, *J* 2.4 Hz), 7.77 (d, 1H, *J* 8.7 Hz); HRMS (ESI) calc. for $C_{11}H_{10}Cl_2N_4NaO_2$ 323.0079, found $[M+Na]^+$ 323.0057. Δ 6.8 ppm.

Ethyl 5-amino-1-(4-nitrophenyl)-1H-1,2,3-triazole-4-carboxylate (**16i**). 87% yield. m.p.: 126–127 °C (lit. [38] 124–125 °C); ^{1}H NMR (300.00 MHz, DMSO-d_6, TMS, δ ppm): 1.33 (t, 3H, *J* 7.1 Hz), 4.33 (q, 2H, *J* 7.1 Hz), 6.70 (s, 2H), 7.91 (d, 2H, *J* 8.9 Hz), 8.43 (d, 2H, *J* 8.9 Hz); HRMS (ESI) calc. for $C_{11}H_{11}N_5NaO_4$ 300.0709, found $[M+Na]^+$ 300.0703. Δ 2.0 ppm.

2.1.2. General procedure for obtaining ethyl 5-(phenylamino)2H-1,2,3-triazole-4-carboxylates **17a-i**

A mixture of 1*H*-1,2,3-triazoles **16a-i** (0.32 mmol) were refluxed for 3 h in pyridine (8 mL, 10 mmol) to promote Dimroth rearrangement. The reaction mixture was poured into 50 mL of ice water. The precipitate that formed was collected by filtration and washed with a lot of water to remove pyridine to obtain **17a-i** with yields of 85–95%.

Ethyl 5-((phenyllamino)–2H-1,2,3,-triazole-4-carboxylate (**17a**). 85% yield. m.p.: 137–138 °C; ^{1}H NMR (300.00 MHz, DMSO-d_6, TMS, δ ppm): 1.34 (t, 3H, *J* 7.1 Hz), 4.36 (q, 2H, *J* 7.1 Hz), 6.91 (t, 1H, *J* 7.3 Hz), 7.31–7.27 (m, 2H), 7.54 (d, 2H, *J* 7.7 Hz), 7.98 (s, 1H); ^{13}C NMR (125.0 MHz, DMSO-d_6, TMS, δ ppm): 14.1, 60.5, 116.7, 120.7, 124.4, 128.9 129.8, 140.8, 161.8; HRMS (ESI) calc. for $C_{11}H_{12}N_4NaO_2^+$ 255.0852, found $[M+Na]^+$ 255.0852. Δ 0 ppm.

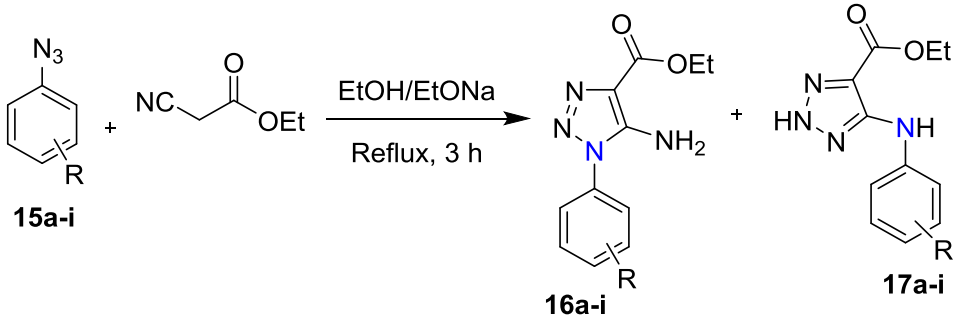

Scheme 1. Synthesis of 1,2,3-triazoles **16** and **17**.

Table 1
Yields found for compounds **16** and **17** under conditions reflux in ethanol.

R	Compounds	Yields	Compounds	Yields
H	**16a**	33%	**17a**	–
4-CH_3	**16b**	31%	**17b**	–
4-OCH_3	**16c**	33%	**17c**	–
4-F	**16d**	30%	**17d**	32%
4-Cl	**16e**	37%	**17e**	30%
4-Br	**16f**	30%	**17f**	35%
2-Cl	**16g**	–	**17g**	46%
2,5-*di*Cl	**16h**	–	**17h**	50%
4-NO_2	**16i**	–	**17i**	55%

Ethyl 5-((p-tolyl)amino)–2H-1,2,3,-triazole-4-carboxylate (**17b**). 86% yield. m.p.: 129–130 °C; ^{1}H NMR (300.00 MHz, DMSO-d_6, TMS, δ ppm): 1.33 (t, 3H, *J* 7.1 Hz), 2.24 (s, 3H), 4.35 (q, 2H, *J* 7.1 Hz), 7.10 (d, 2H, *J* 8.2 Hz), 7.42 (d, 2H, *J* 8.4 Hz), 7.94 (s, 1H); ^{13}C NMR (125.0 MHz, DMSO-d_6, TMS, δ ppm): 14.1, 20.2, 60.5, 116.9, 124.4, 129.3, 129.6, 138.4, 149.8, 161.9; HRMS (ESI) calc. for $C_{12}H_{14}N_4NaO_2^+$ 269.1014, found $[M+Na]^+$ 269.1006. Δ 3.0 ppm.

Ethyl 5-((4-methoxyphenyll)amino)–2H-1,2,3,-triazole-4-carboxylate (**17c**). 90% yield. m.p.: 145–146 °C; ^{1}H NMR (300.00 MHz, DMSO-d_6, TMS, δ ppm): 1.32 (t, 3H, *J* 7.1 Hz), 3.71 (s, 3H), 4.34 (q, 2H, *J* 7.1 Hz), 6.88 (d, 2H, *J* 9.0 Hz), 7.44 (d, 2H, *J* 8.9 Hz), 7.84 (s, 1H); ^{13}C NMR (125.0 MHz, DMSO-d_6, TMS, δ ppm): 14.1, 55.3, 60.4, 114.3, 114.9, 118.8, 126.4, 134.2, 146.3, 159.9; HRMS (ESI) calc. for $C_{12}H_{14}N_4NaO_3^+$ 285.0958, found $[M+Na]^+$ 285.0948. Δ 3.5 ppm.

Ethyl 5-((4-fluorophenyll)amino)–2H-1,2,3,-triazole-4-carboxylate (**17d**). 90% yield. m.p: 133–134 °C; IR (KBr, cm^{-1}): 3382–3144, 2980–2902, 1693, 1613–1550, 1276, 821–781; ^{1}H NMR (300.00 MHz, DMSO-d_6, TMS, δ ppm): 1.33 (t, 3H, *J* 7.1 Hz), 4.36 (q, 2H, *J* 7.1 Hz), 7.15 (t, 2H, *J* 8.9 Hz), 7.59 (dd, 2H, *J* 9.1 and 4.7 Hz), 8.03 (s, 1H); ^{13}C NMR (125.0 MHz, DMSO-d_6, TMS, δ ppm): 13.9, 60.4, 115.1 (d, $^2J_{C\text{-}F}$ 22.4 Hz), 118.4 (d, $^3J_{C\text{-}F}$ 7.5 Hz), 137.2 (d, $^1J_{C\text{-}F}$ 1.5 Hz), 155.2, 158.3, 161.6; HRMS (ESI) calc. for $C_{11}H_{12}FN_4O_2$ 251.0944, found $[M + H]^+$ 251.0935. Δ 3.6 ppm.

Ethyl 5-((4-chlorophenyl)amino)–2H-1,2,3,-triazole-4-carboxylate (**17e**). 95% yield. m.p: 157–159 °C; IR (KBr, cm^{-1}): 3373–3072, 2998–2932, 1700, 1615–1577, 1276, 814–783; ^{1}H NMR (300.00 MHz, DMSO-d_6, TMS, δ ppm): 1.35 (t, 3H, *J* 7.1 Hz), 4.38 (q, 2H, *J* 7.1 Hz), 7.31 (d, 2H, *J* 8.9 Hz), 7.58 (d, 2H, *J* 8.9 Hz), 8.12 (s, 1H); ^{13}C NMR (125.0 MHz, DMSO-d_6, TMS, δ ppm): 14.5, 61.0, 118.8, 124.7, 129.0, 140.5; HRMS (ESI) calc. for $C_{11}H_{11}ClN_4NaO_2$ 289.0468, found $[M+Na]^+$ 289.0464. Δ 1.4 ppm.

Ethyl 5-((4-bromophenyl)amino)–2H-1,2,3,-triazole-4-carboxylate (**17f**). 93% yield. m.p: 164–165 °C; IR (KBr, cm^{-1}): 3378–3070, 2997, 2927, 1696, 1607, 1571, 1271, 1111, 811–783; ^{1}H NMR (300.00 MHz, DMSO-d_6, TMS, δ ppm): 1.34 (t, 3H, *J* 7.1 Hz), 4.37 (q, 2H, *J* 7.1 Hz), 7.43 (d, 2H, *J* 9.0 Hz), 7.53 (d, 2H, *J* 9.0 Hz), 8.12 (s, 1H); ^{13}C NMR (125.0 MHz, DMSO-d_6, TMS, δ ppm): 13.9, 60.3, 111.6, 118.5, 122.3, 131.2, 140.3, 149.2, 161.4; HRMS (ESI) calc. for $C_{11}H_{12}BrN_4NaO_2$ 332.9963, found $[M+Na]^+$ 332.9946. Δ 5.1 ppm.

Ethyl 5-((2-chlorophenyl)amino)–2H-1,2,3,-triazole-4-carboxylate (**17g**). 87% yield. m.p: 266–266 °C; IR (KBr, cm^{-1}): 3542–3384, 2984, 1698, 1596–1556, 781–700; ^{1}H NMR (300.00 MHz, DMSO-d_6, TMS, δ ppm): 1.32 (t, 3H, *J* 7.1 Hz), 4.25 (q, 2H, *J* 7.1 Hz), 6.76–6.72 (m, 1H), 7.26–7.22 (m, 2H), 7.34 (dd, 1H, *J* 7.9 and 1.5 Hz), 8.35 (s, 1H), 8.78 (dd, 1H, *J* 8.3 and 1.6 Hz); ^{13}C NMR (125.0 MHz, DMSO-d_6, TMS, δ ppm): 14.4, 58.3, 116.4, 118.0, 118.5, 120.4, 127.5, 128.3, 139.0, 150.6, 163.8; HRMS (ESI) calc. for $C_{11}H_{11}ClN_4NaO_2$ 289.0468, found $[M+Na]^+$ 289.0458. Δ 3.4 ppm.

Ethyl 5-((2,5-dichlorophenyl)amino)–2H-1,2,3,-triazole-4-carboxylate (**17h**). 92% yield. m.p: 128–219 °C; IR (KBr, cm^{-1}): 3379–3287, 2978, 1689, 1596–1549, 1689, 779–695; ^{1}H NMR (300.00 MHz, DMSO-d_6, TMS, δ ppm): 1.37 (t, 3H, *J* 7.1 Hz), 4.41 (q, 2H, *J* 7.1 Hz), 7.02 (dd, 1H, *J* 8.5 and 2.5 Hz), 7.52 (d, 1H, *J* 8.5 Hz), 8.34 (d, 1H, *J* 1.3 Hz), 8.53 (s, 1H); ^{13}C NMR (125.0 MHz, DMSO-d_6, TMS, δ ppm): 14.4, 58.6, 115.4, 116.6, 118.0, 120.6, 129.6, 132.3, 139.7, 150.0, 163.8; HRMS (ESI) calc. for $C_{11}H_{10}Cl_2N_4NaO_2$ 323.0079, found $[M+Na]^+$ 323.0067. Δ 3.7 ppm.

Ethyl 5-((4-nitrophenyl)amino)–2H-1,2,3,-triazole-4-carboxylate (**17i**). 90% yield. m.p: 220–221 °C; IR (KBr, cm^{-1}): 3606–3301, 1672, 1591, 1461, 833–703; ^{1}H NMR (300.00 MHz, DMSO-d_6, TMS, δ ppm): 1.30 (t, 3H, *J* = 7.1 Hz), 4.24 (q, 2H, *J* 7.1 Hz), 7.78 (d, 2H, *J* 9.3 Hz), 8.08 (d, 2H, *J* 9.4 Hz), 8.61 (s, 1H); ^{13}C NMR (125.0 MHz, DMSO-d_6, TMS, δ ppm): 14.0, 60.8, 115.7, 125.3, 139.8, 147.5, 159.6, 161.1, 169.4; HRMS (ESI) calc. for $C_{11}H_{11}N_5NaO_4$ 300.0709, found $[M+Na]^+$ 300.0697. Δ 4.0 ppm.

2.1.3. 2.1.3. Alternative Condition: General procedure for obtaining ethyl 5-amino-1-phenyl-1H-triazole-4-carboxylates *16a-i* and ethyl 5-(phenylamino)2H-1,2,3-triazole-4-carboxylate *17a-i*

A mixture of arilazide (**15a-i**, 0.01 mol) and ethyl cyanoacetate (0.01 mol) in 25 mL of dry ethanol containing 0.01 mol of sodium ethoxide was kept under stirring at reflux in inert atmosphere for three hours. The reaction mixture was poured into 50 mL of ice water. The precipitate that formed was collected by filtration and washed with water to obtain **17a-i**. The residual ethanol that remained in the solution was evaporated and the residue was extracted with ethyl acetate, dried with anhydrous sodium sulfate and after evaporation, a solid was obtain that was purified dissolving them in chloroform at room temperature and precipitation with petroleum ether, these solids were identified as being substances **16a-i**.

2.1.4. General procedure for obtaining of *18*

The derivative **17e** (4 mmol) was reacted with 5 mL of acetic acid, 0,25 mL of pyridine and DMAP in catalytic quantity. The reaction was kept under stirring at room temperature for approximately 24 h. After that time, the mixture was poured into water and extracted with dichloromethane. The organic phase was dried with anhydrous sodium sulfate, filtered and the solvent evaporated to obtain **18**.

Ethyl 2-acetyl-5-((4-chlorophenyl)amino)–2H-1,2,3-triazole-4-carboxylate (**18**). 50% yield. m.p: 143–143 °C; IR (KBr, cm^{-1}): 3348, 2983,

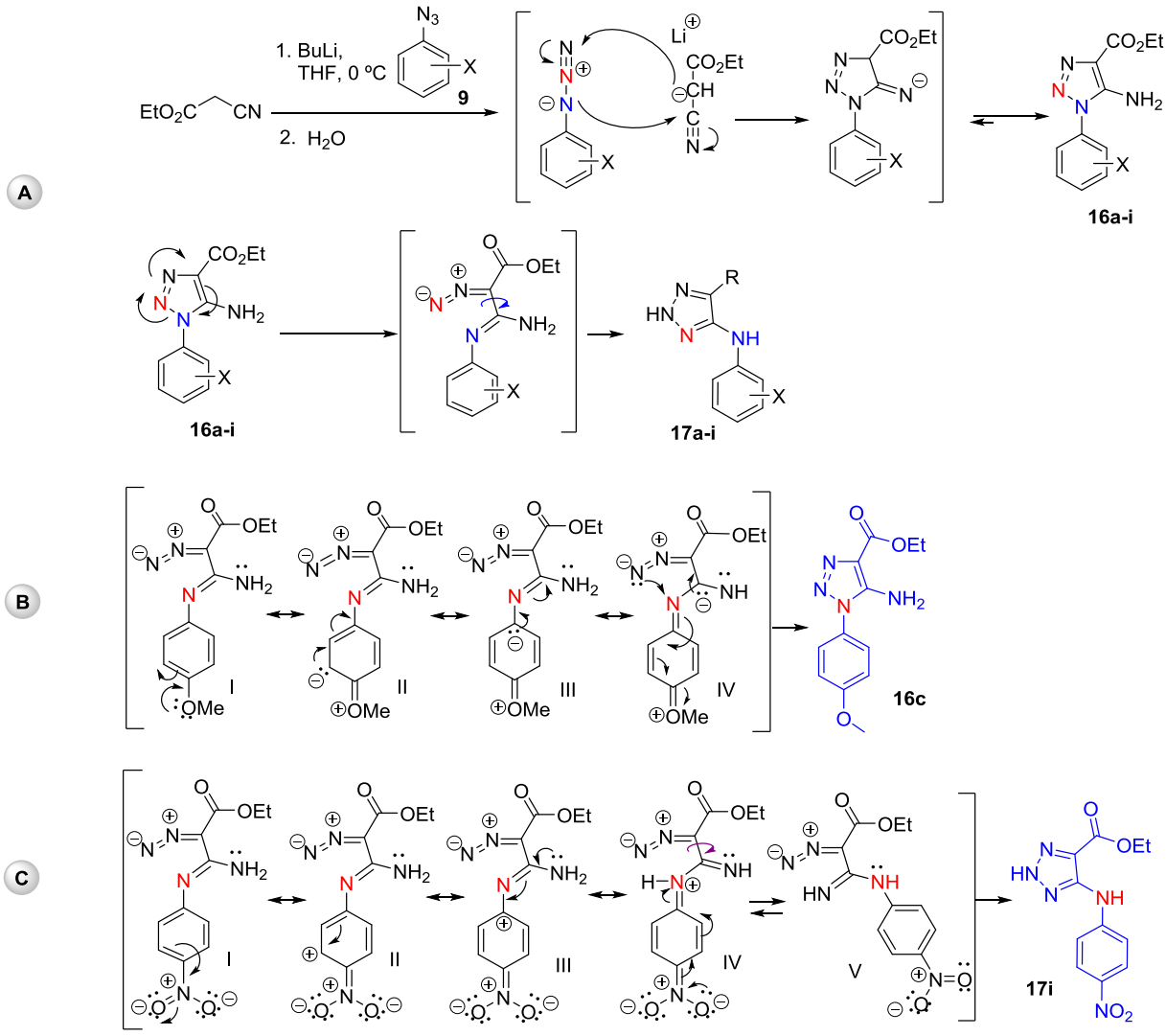

Scheme 2. Proposed scheme of intermediates and effects of substituents for the derivatives **16c** and **17i**.

Table 2
Yields found for the triazoles **16** under rt conditions in ethanol and later obtaining **17** in reflux of pyridine.

R	Compounds	Yields	Compounds	Yields
H	**16a**	62%	**17a**	85%
4-CH_3	**16b**	65%	**17b**	86%
4-OCH_3	**16c**	67%	**17c**	90%
4-F	**16d**	60%	**17d**	90%
4-Cl	**16e**	60%	**17e**	95%
4-Br	**16f**	93%	**17f**	93%
2-Cl	**16g**	56%	**17g**	87%
2,5-*di*Cl	**16h**	65%	**17h**	92%
4-NO_2	**16i**	87%	**17i**	90%

2930, 1750, 1694, 1595–1564, 1239, 833–791; ^{1}H NMR (300.00 MHz, DMSO-d_6, TMS, δ ppm): 1.40 (t, 3H, *J* 7.1 Hz), 2.76 (s, 3H), 4.44 (q, 2H, *J* 7.1 Hz), 7.32 (d, 2H, *J* 8.9 Hz), 7.53 (d, 2H, *J* 9.0 Hz), 8.12 (s, 1H); ^{13}C NMR (125.0 MHz, DMSO-d_6, TMS, δ ppm): 14.3, 22.1, 62.6, 118.6, 127.2, 129.3, 129.4, 137.9, 151.5, 162.5, 165.6; HRMS (ESI) calc. for $C_{13}H_{13}ClN_4NaO_3$ 331.0574, found $[M+Na]^+$ 331.0587. Δ 3.9 ppm.

2.1.5. General procedure for obtaining of 19

The derivative **16d** (4 mmol) was reacted with 5 mL of acetic acid, 0,25 mL of pyridine and DMAP in catalytic quantity. The reaction was kept under stirring at room temperature for approximately 24 h. After that time, the mixture was poured into water and extracted with dichloromethane. The organic phase was dried with anhydrous sodium sulfate, filtered and the solvent evaporated to obtain **19**.

Ethyl 5-(N-acetylacetamido)-1-(4-fluorophenyl)-1H-1,2,3-triazole-4-carboxylate (**19**). 58 % yield. m.p: 102–103 °C; IR (KBr, cm^{-1}): 338–3139, 2981, 2906, 1692, 1583, 1520, 852–779; ^{1}H NMR (300.00 MHz, DMSO-d_6, TMS, δ ppm): 1.44 (t, 3H, *J* 7.1 Hz), 2.27 (s, 6H), 4.44 (q, 2H, *J* 7.1 Hz), 7.24 (t, 2H, *J* 5.0 Hz), 7.47 (dd, 2H, *J* 9.0 and 4.6 Hz); ^{13}C NMR (125.0 MHz, DMSO-d_6, TMS, δ ppm): 14.3, 25.8, 62.0, 117.4 (d, $^2J_{C\text{-}F}$ 23.4 Hz), 126.64 (d, $^3J_{C\text{-}F}$ 9.0 Hz), 129.9 (d, $^4J_{C\text{-}F}$ 3.1 Hz), 134.5, 137.7, 159.8 (d, $^1J_{C\text{-}F}$ 277.6 Hz), 165.0, 171.1; HRMS (ESI) calc. for $C_{15}H_{15}FN_4NaO_4$ 357.0975, found $[M+Na]^+$ 357.0982. Δ 2.0 ppm.

2.1.6. Crystallographic data

Crystallographic data for compound **17f**: $C_{11}H_{11}BrN_4O_2$, F.W. 311.15, light yellow block, monoclinic, space group $P2_1/n$, a = 10.8885 (4) Å, b = 21.4709(7) Å, c = 16.4204(6) Å, β = 100.580(2)°, volume = 3773.6(2) Å^3, Z = 12, ρ_c = 1.643 g/cm^3, μ = 3.268 mm^{-1}, F(000) = 1872, Crystal dimensions: 0.221 × 0.141 × 0.114 mm^3. Independent reflections: 6899 (R_{int} = 0.118). The final anisotropic full-matrix least-squares refinement on F^2 with 492 variables converged at R_1 = 5.74 %, for the observed data; wR_2 = 15.15 % for all data and Goodness-of-fit on F^2 = 1.067. CCDC number: 2004004.

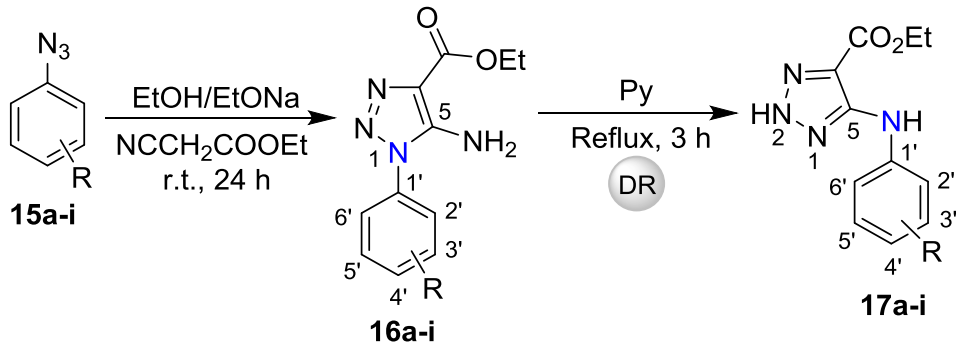

Scheme 3. Synthesis of triazoles **16a-i** and **17a-i**.

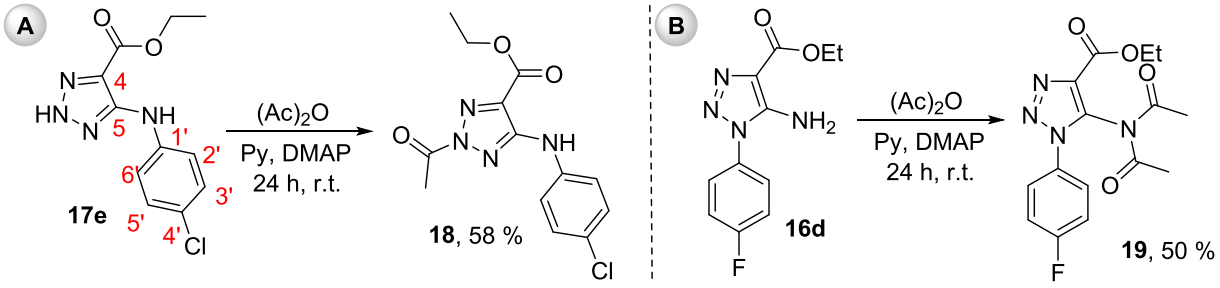

Scheme 4. Acetylation of compounds **17e** (A) and **16d** (B).

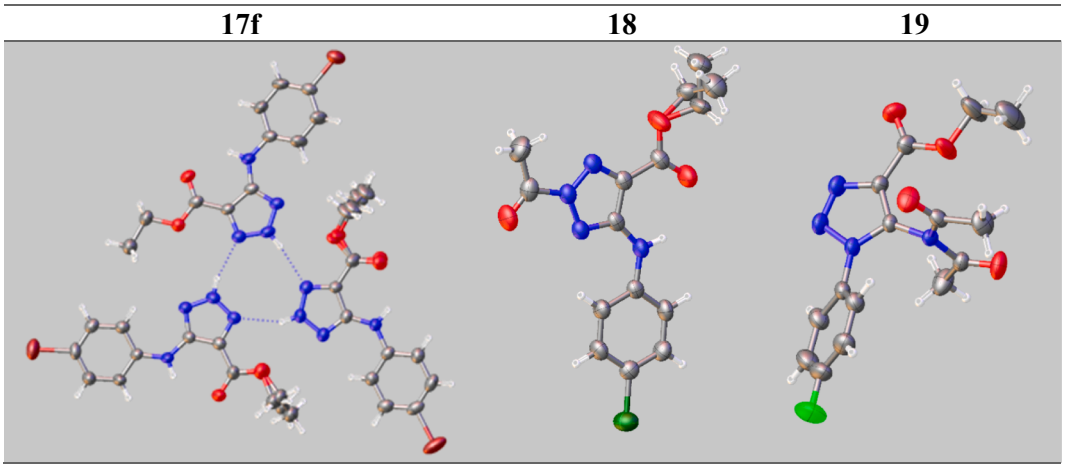

Fig. 3. A) 2D NMR correlations and ORTEP-3 representation of compound **17f**; B) asymmetric unit representation of 1*H*-1,2,3-triazoles *N*-acetylated **18** and C) asymmetric unit representation of 2*H*-1,2,3-triazoles *N,N*-diacetylated **19**. Displacement ellipsoids are drawn at the 50% probability level.

Crystallographic data for compound **18**: $C_{15}H_{15}FN_4O_4$, F.W. = 334.31, colorless plate, triclinic, space group *P*-1, a = 7.8424(11) Å, b = 8.8306(11) Å, c = 12.1432(17) Å, α = 98.544(4)°, β = 91.609(4)°, γ = 110.202(4)°, volume = 777.60(18) Å^3, Z = 2, ρ_c = 1.428 g/cm^3, μ = 0.114 mm^{-m}, F(000) = 348, Crystal dimensions: 0.25 × 0.16 × 0.08 mm^3. Independent reflections: 2855 (R_{int} = 0.092). The final anisotropic full-matrix least-squares refinement on F^2 with 220 variables converged at R_1 = 6.22%, for the observed data; wR_2 = 0,1512 % for all data and Goodness-of-fit on F^2 = 1.035. CCDC number: 2004002.

Crystallographic data for compound **19**: $C_{13}H_{13}ClN_4O_3$, F.W. = 308.72, colorless plate, monoclinic, space group *C*2/*c*, a = 23.6589(10) Å, b = 8.9350(4) Å, c = 17.2063(12) Å, β = 128.3990(10)°, volume = 2850.5(3) Å^3, Z = 8, ρ_c = 1.439 g/cm^3, μ = 0.284 mm^{-1}, F(000) = 1280, Crystal dimensions: 0.3 × 0.178 × 0.09 mm^3. Independent reflections: 2612 (R_{int} = 0.091). The final anisotropic full-matrix least-squares refinement on F^2 with 212 variables converged at R_1 = 4.70%, for the observed data; wR_2 = 11.90% for all data and Goodness-of-fit on F^2 = 1.066. CCDC number: 2004003.

2.2. Biological assays

2.2.1. Cytotoxicity assay in mammalian cells

Mice peritoneal macrophages collected from male Swiss mice through the peritoneal cavity lavage using 10 mL of Dulbecco's modified Eagle's medium (DMEM) medium. The collected cell suspension was centrifuged at 1500 rpm for 5 min and this content suspended in 1 mL of Roswell Park Memorial Institute (RPMI) 1640 supplemented with 10% inactivated FBS. Cells were plated on 96-well flat-bottom microplates at a density of 4 × 10^5 macrophages/well in triplicates. These plates were maintained for cell adhesion in a humidified atmosphere (37 °C, 5% CO_2). After 24 h, the cell medium was replaced and for a new medium with tested compounds diluted in DMEM without fetal bovine serum for

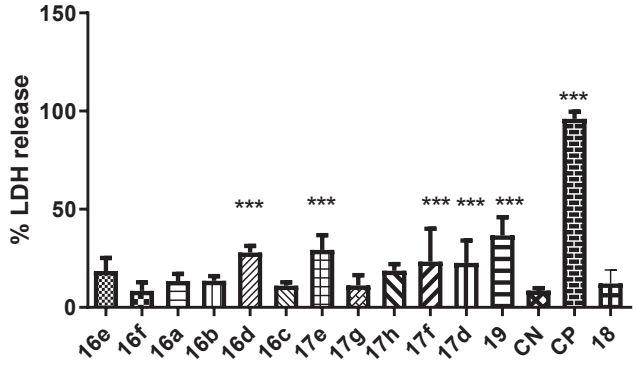

Fig. 4. LDH release test in peritoneal macrophages. Incubation time 24 h. This test was repeated four times in 4 different days. CN - untreated cells, CP - cells treated with 0.05% Tx100. *** $p < 0.05$ when compared to CN (negative control).

24 h. We tested the drug concentrations of 10 nM, 100 nM, 1 μM, 25 μM, 50 μM, and 100 μM. Culture medium was used as a negative control, and 0.5% Triton X-100 as a positive control. Cell viability was evaluated using LDH release kit (Promega) according to the manufacturer's instructions. The cell supernatants were tested for LDH, which reduces NAD^+, which in turn converts tetrazolium dye into a soluble, colored formazan derivative. The absorbance readings were performed in a spectrophotometer M5 (Molecular Devices) at 490 nm, using the SoftMax Pro (version 5.1). Cytotoxicity was expressed as the percentage of cells surviving after treatment with samples in comparison to untreated cells.

2.2.2. Evaluation of antitrypanosomal activity

Epimastigotes forms of Y strain from *T. cruzi* was cultured in medium LIT (Tryptose Liver infusion) supplemented with 10% fetal calf serum, at a temperature of 28 °C, with strong agitation (100 rpm). Epimastigotes plated into 96-well flat-bottom microplates at a quantity of 5×10^5 cells/100 μL treated with 10 μM benznidazole or triazole analogs (1 nM to 100 μM), and incubated for 72 h at 37 °C in a humidified atmosphere of 5% CO_2. Drugs or vehicle (dimethyl sulfoxide [DMSO]) was added after 24 h under each condition. Triazole analogs were tested at least for three independent experiments in triplicate. A solution containing 10% Alamar Blue® (AbD Serotec, Raleigh, North Carolina) was added to wells after 56 h and the fluorescence recorded in the point of 72 h. Prisma GraphPad 5.0 was used for calculating the effective concentration able to give death of 50% of parasites (EC_{50}). The fluorescence was measured in the Spectramax M5 microplate fluorometer (Molecular Devices) with a 530 nm excitation and 590 nm emission wavelengths.

2.2.3. Evaluation of trypanocide action on trypomastigote forms

Trypomastigotes forms were collected from the blood samples of infected Swiss Webster mice at the peak of parasitemia. The purified parasites were suspended in DMEM supplemented with 10% FBS. Vero cells were maintained in RPMI supplemented with 5% FBS, 100 UI/mL of antibiotics mixture, 10 μg/mL streptomycin at 37 °C in an atmosphere of 5% CO_2. The cell monolayer (90% of confluence) was infected with trypomastigotes (Y strain, 10 parasites per cell). We collected the supernatant after 24 h, and Vero cells and amastigotes were discarded for centrifugation at 1000*g* by 5 min. Trypomastigotes were collected by centrifugation at 1600*g* by 10 min. It was used in tests 1×10^6 trypomastigotes/mL in 96-well plattes incubated at 37 °C for 24 h in the presence of drugs. Trypomastigote viability was quantified by counting in a Neubauer chamber.

2.2.4. Evaluation of trypanocidal activity

For evaluation of trypanocidal activity, cells were seeded into 96-well flat-bottom microplates at a density of 1×10^6 cells/100 μL in the presence of benznidazole or tested compounds (1 μM). Propidium iodide (750 nM) was added to each treated well during the last 30 min of incubation at 28 °C. The fluorescence pattern was analyzed using a spectrophotometer SpectraMax M5 (Molecular Devices) at 565–605 nm wavelength. Triton X-100 was used as a positive control of trypanocidal activity and untreated cells were used as negative control. All experiments were performed in triplicates.

2.2.5. Spectroscopic $CYP51_{TC}$ binding assay

Recombinant $CYP51_{Tc}$ was produced as depicted elsewhere [40]. Binding assays were realized by spectrophotometric titration with 3 mL of 50 mM Tris-HCl (pH 7.5) and 10% glycerol, using a UV–visible (UV–vis) scanning spectrophotometer (Varian). The $CYP51_{Tc}$ concentration was 0.1 μM. A stock solution of **16d**, **16f**, and **17d** were dissolved in DMSO at 20 μM. Titrations were conducted using a 3.5-mL quartz cuvette with a path length of 1 cm, and the inhibitor was added in 300 μL aliquots. As a negative control, DMSO was added in the same amounts of, followed by recording of difference spectra. K_D (dissociation constant) values were determined for titration of data points fitted to quadratic hyperbola using GraphPad PRISM software (GraphPad Software Inc.), as follows: $A_{obs} = (A_{max}/2 \times E_t)\{(S + E_t + K_D) - [(S + E_t + K_D)^2 - 4 \times S \times E_t]^{0.5}\}$, where A_{obs} is the absorption change determined at any inhibitor concentration, A_{max} is the maximal absorption shift recorded at saturation, K_D is the dissociation constant for the inhibitor-

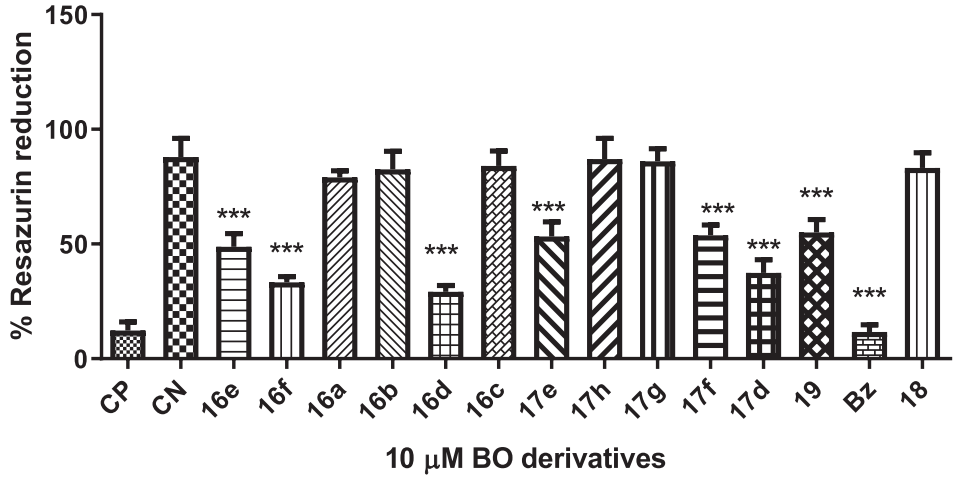

Fig. 5. Assay of cellular metabolic activity by reducing resazurin in *Trypanosoma cruzi* Y strain epimastigotes. Incubation time 72 h. This test was repeated four times in 4 different days. CN - untreated cells, CP - cells treated with 0.05% Tx100. *** $p < 0.05$ when compared to CN (negative control).

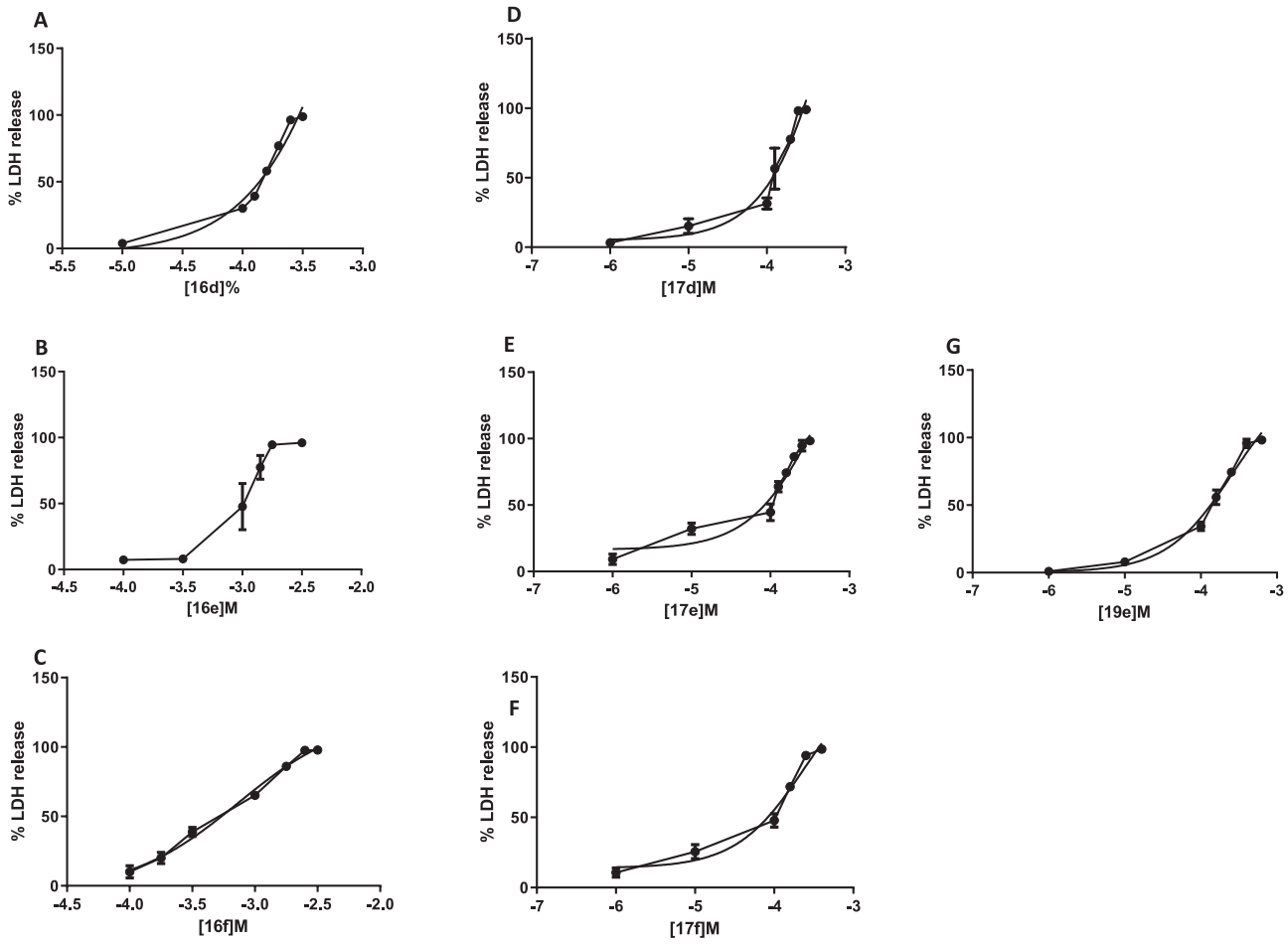

Fig. 6. LDH release test in peritoneal macrophages. The cells were incubated with analogs for 24 h. The triazole analogs were tested in concentrations from 1 μM to 5000 μM. (A) **16d**, (B) **16e**, (C) **16f**, (D) **17d**, (E) **17e**, (F) **17f**, (F) **19**. This test was repeated four times in 4 different days.

enzyme complex, E_t is the total enzyme concentration used, and S is the inhibitor concentration.

2.2.6. *In silico studies*

The compounds of the series triazoles **16** and **17** and compounds **11b** and **11c** were initially built using the program Avogadro [30,41]. Then, the geometry optimizations of molecules were performed using the MMFF94 force field [42]. The optimized conformers were submitted to refinement calculations of the geometry optimization using the semi-empirical method PM6 performed by program MOPAC2016 [43,44].

2.2.7. *Molecular docking*

The molecular docking was performed using the Molegro Virtual Docker (MVD) 6.0 program (CLC Bio, 8200, Aarhus, Denmark) [45]. The MolDock score algorithm [GRID] with a grid resolution of 0.30 Å was selected as the score function, and the partial charges were assigned according to the MVD charges scheme. The MolDock Optimizer algorithm was used with a search space of 32 Å around of *T. cruzi* protein CYP51 structure. Molecular redocking was performed with four different inhibitors of CYP51, validating the approach by the root mean square deviation (RMSD). Molecular complexes applied in redocking were retrieved from Protein Data Bank (PDB). Molecular docking of the TD series compounds and triazole derivatives **11b** and **11c** was performed using the same parameters set (runs = 100, population size = 50, max interactions = 2000, scaling factor = 0.50, and crossover rate = 0.90) and ligands poses were selected based on MolDock score values. Both programs Molegro Virtual Docker (MVD) 6.0 program (CLC Bio, 8200, Aarhus, Denmark) and Pymol (The PyMOLMolecular Graphics System, Version 2.0 Schrödinger, LLC) were used to visualize and analyze the optimized molecular complexes.

2.2.8. *Protein/ligand binding enthalpy*

Enthalpy is the binding process that indicates the energy variation of the molecular system when the ligand binds to the protein [46]. Molecular complexes obtained by docking and separate optimized ligands with protein before docking were applied to MOZYME calculation using constant dielectric 78.4 in order to indicate the molecular systems heat of formation (ΔH_f) by program MOPAC2016 [47,48]. Protein and heme group atoms coordinates were fixed, and for ligands, the geometry optimization was allowed freely.

3. Results and discussion

Our research group reported the synthesis of several triazole derivatives as potent inhibitors of *T. cruzi* [30]. Continuing these studies, other triazole derivatives, 5-amino-1H-triazole and 5-(arylamino)–2*H*-1,2,3-triazole, were synthesized and biologically evaluated against *T. cruzi*.

3.1. *Chemistry*

Initially, arylazides **15a-i** were prepared in quantitative yields from commercial anilines through their treatment with sodium nitrite in hydrochloric acid at 0–5 °C followed by aromatic electrophilic substitution with sodium azide (Scheme 1) [49,50]. Then, when arylazides **15a-i** were reacted with ethyl cyanoacetate in the presence of sodium ethoxide

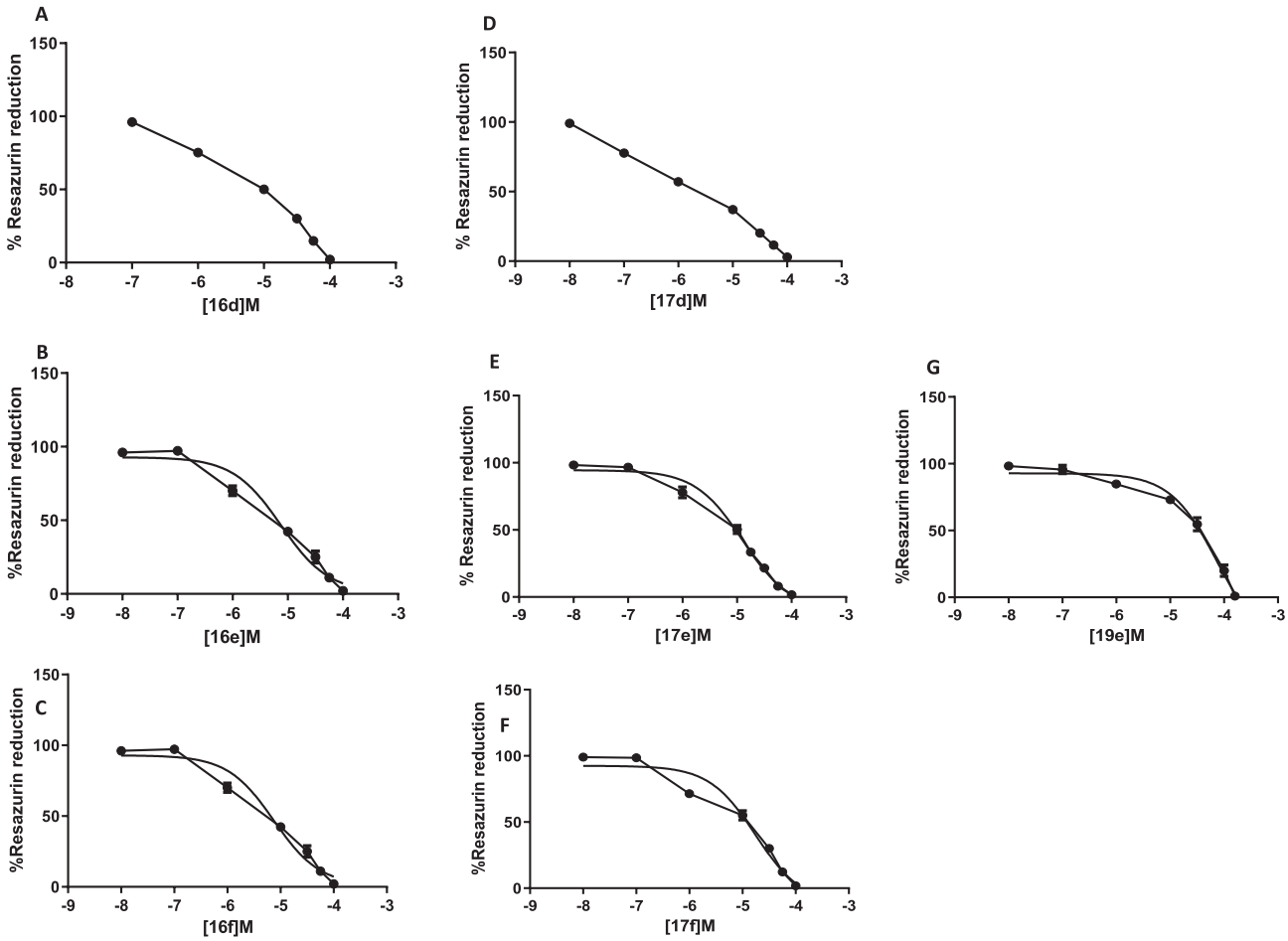

Fig. 7. Assay of cellular metabolic activity by reducing resazurin in Trypanosoma cruzi Y strain epimastigotes. The parasites were incubated with analogs for 72 h. The triazole analogs were tested in concentrations from 10 nM to 100 μM. (A) **16d**, (B) **16e**, (C) **16f**, (D) **17d**, (E) **17e**, (F) **17f**, (F) **19**. This test was repeated at least three times in 3 separate days.

and etanol under reflux for 3 h, triazoles **16** and **17** were formed (Scheme 1). We observed that when R group is an electronic donor or hydrogen substituent, only triazoles **16** is formed. Halogens at position C-4 of the phenyl ring result in a mixture of products **16** and **17**. The nitro group at the C-4 or chlorine at C-2 and C-5 position of the phenyl ring, provide only the triazoles **17**. The products were isolated, and the yields are showed in Table 1.

In Scheme 2**A, a** scheme of intermediates of the cycloaddition reaction and subsequent Dimroth rearrangement leading to products **16** and **17** respectively is proposed. We can see the resonance structures for the formation of derivative **16c**, with R is 4-OCH_3, a strong electron donor group (ERG), due to generation a negative charge on the neighbor carbon to NH_2, making it difficult to transfer the proton to the phenyl-bound nitrogen (Scheme 2**B**). On the other hand, the formation of derivative **17i**, R is 4-NO_2, a strong electron withdrawer group (EWG), is favored by the transfer of the proton and lower electronic density, absence of negative charge at carbon-azo (anomeric type), enabling rotation (Scheme 2**C**).

To obtain derivatives **16** and **17** in higher yields, sequential synthesis was carried out in two stages: synthesis of 5-amino-1*H*-triazoles derivatives **16a-i** and then their conversion to 5-(arylamino)–2*H*-1,2,3-triazole **17a-i**. The synthesis of the 5-amino-1*H*-triazoles derivatives **16a-i** was carried out from the respective arylazides **15a-i** which were reacted with ethyl cyanoacetate in the presence of sodium ethoxide in ethanol at room temperature for 24 h. The amine compounds were obtained in good yields that ranged from 56 to 93% (Table 2). As it is known that the Dimroth rearrangement is favored under heating, the amino compounds **16a-i** were refluxed in pyridine for 3 h. Compounds **17a-i** were obtained in excellent yields ranging from 85 to 95% (Table 2), confirming that the basic medium and the high temperature favor the formation of the products *via* Dimroth rearrangement (Scheme 3).

All compounds **16a-i** and **17a-i** had their structures confirmed by physical methods of analysis (See SI). Derivatives **16a-i** are already described in the literature [37-39]. However, 2*H*-1,2,3-triazoles **17a-i** are being reported for the first time, since these structures are described to be 1*H*-1,2,3-triazoles [51-54] Illustratively, compound **17f** had its structure confirmed by 1H NMR spectrum in 2D - HMBC, which showed a correlation between the hydrogen of N—H group and three carbons present in the benzene ring: $^{2}J_{C\text{-}H}$=C-1′(N—H), $^{3}J_{C\text{-}H}$=C-2′(N—H) and $^{3}J_{C\text{-}H}$=C-6′(N—H). However, the position of hydrogen in the triazole ring could not be confirmed by spectroscopy techniques.

To obtain information about which tautomer was preferentially formed, an acetylation reaction of triazole **17e** was carried out (Scheme 4A). The reaction took place in the presence of acetic anhydride, pyridine and catalyzed by DMAP resulting in the acetylated derivative **18** in 58% yield (part of the starting material was recovered). It is interesting to note that when the 5-amino-triazole derivative **16d** was subjected to an acetylation under the same reaction conditions a diacetylated derivative **19** was obtained in 50% yield (Scheme 4B). The *N,N*-diacetylation is known in the literature, and its mechanism was proposed by Ayyangar and Srinivasan [55].

The monocrystal X-ray diffraction analysis of compound **18** (Fig. 3**B**) showed that the acetyl group was incorporated exactly in N-2 position of

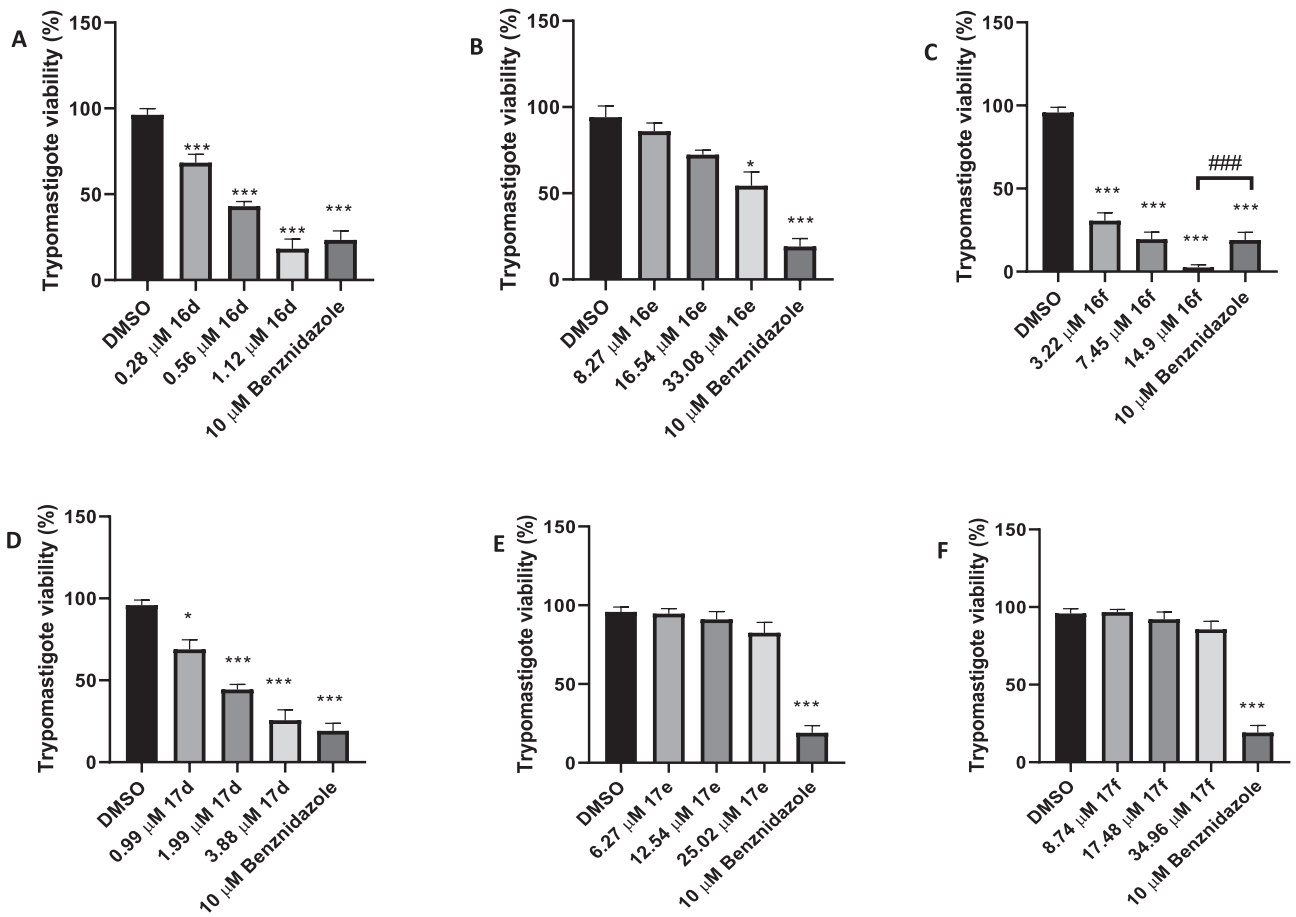

Fig. 8. Toxicity test on *Trypanosoma cruzi* trypomastigotes. The trypomastigotes were incubated with analogs for 24 h. This test was repeated three times on two separate days. DMSO - untreated cells, *** $p < 0.05$ when compared to the DMSO group (negative control). ### $p < 0.05$ when compared to the Benznidazole group.

Table 3
SI of compounds more activities.

Drugs	CC_{50} (μM) *Peritoneal Macrophages*	EC_{50} (μM) Y strain	SI
16d	129,5	0,56	231
16e	1539	16,54	93
16f	7284	7,45	977
17d	1144	1,99	575
17e	422,3	12,54	34
17f	247,4	17,48	14
19	259,6	73,53	3,53
Benznidazol	16.1 ± 2.6	150 ± 5.76	9,33

the triazole ring. The unique formation of this product indicate that N-2 is sterically less hindered and more nucleophilic than the other nitrogen connected in C-5. The monocrystal X-ray diffraction analysis of compound **19** was also performed (Fig. 3**C**). The ortep structure shows that the two acetyl groups were inserted in the same nitrogen atom of the NH_2 group, highly nucleophilic. To definitively prove the exact structure of the tautomer, monocrystal X-ray diffraction analysis of compound **17f** was performed (Fig. 3**A**). The result showed that **17f** is the tautomer 2*H*-1,2,3-triazole with a trimer arrangement in the crystal. Compound **17f** crystallized with three independent molecules in the asymmetric unit. Intermolecular interactions and occupational disorders are major differences between the molecules in the asymmetric unit. Goddard and coworkers determined the crystal structure of unsubstituted 1,2,3-triazole and found that the crystal is a 1:1 mixture of 1*H*- and 2*H*-tautomers [56]. However, when substituted with the phenyl group the triazoles crystallize as 2*H*-tautomer [57].

3.2. Biological assays

The compounds **16**, **17**, **18** e **19** were tested concerning potential trypanocidal activity against *Trypanosoma cruzi*. Initially, the cell toxicity test was performed in vitro using the Lactate Dehydrogenase (LDH) release technique, where the activity of this intracellular enzyme is only measured when damage to the plasma membrane and subsequent extravasation of the cytoplasmic content. Consequently, after the rupture of the plasma membrane, the cell dies from necrosis. Therefore, in the test, treatment was performed with a concentration of 100 μM for all samples, and induction of cell death was observed after 24 h of treatment (Fig. 4) for molecules **16d**, **17d**, **17e**, **17f** and **19**. The highest LDH release value recorded was less than half observed in the positive control (CP). Triton X 100 (0.05%) was used as CP. This detergent ruptures the plasma membrane extravasating the cytoplasmatic content.

The resazurin reduction assay was performed on *T. cruzi* Y strain epimastigotes treated for 72 h. The analogs **16d**, **16e**, **16f**, **17d**, **17e**, **17f**, and **19** at a concentration of 100 μM reduced the viability of the parasites compared to the CN (Fig. 5). Derivatives **16a**, **16b**, **16c**, **17g**, **17h**, **18** were not trypanocidal. In the concentration used, none of the samples had an action superior to the positive controls, 0.05% Triton X-100 (CP), and the benznidazole (100 μM), which is the first choice drug for the Chagas' disease treatment.

Peritoneal macrophages were treated varying concentrations from 1 μM to 5000 μM for 24 h to estimate the CC_{50} value. The CC_{50} value calculated for derivative **16d** obtained a value of 129.5 μM (Fig. 6**A**). Substances **16e** and **16f** obtained CC_{50} values greater than **16e**, respectively, 1539 μM (Fig. 6**B**) and 7284 μM (Fig. 6**C**). The analog **17d** obtained $CC_{50} = 1144$ μM (Fig. 6**D**) and **17e** and **17** had CC_{50} values less

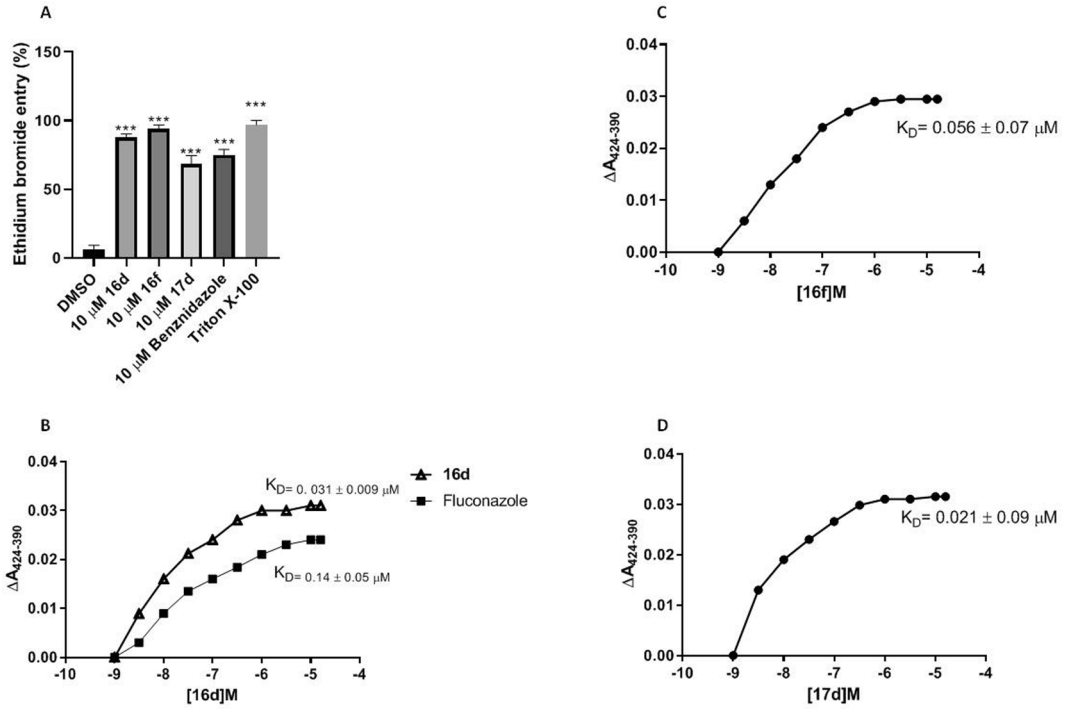

Fig. 9. Triazoles cause cytotoxic effects via CYP51 inhibition. (A) Trypomastigostes were treated for 24 h with analogs or benznidalole, all in the concentration of 10 μM. Triton X-100 (0.05%) and DMSO were used as positive and negative controls, respectively. Compound (B) **16d** and fluconazole (C) **16f** and (D) **17d** binding estimated from the difference absorption variation derived from the titration of CYP51Tc with crescent triazole analogs concentrations. These experiments were realized in triplicate.

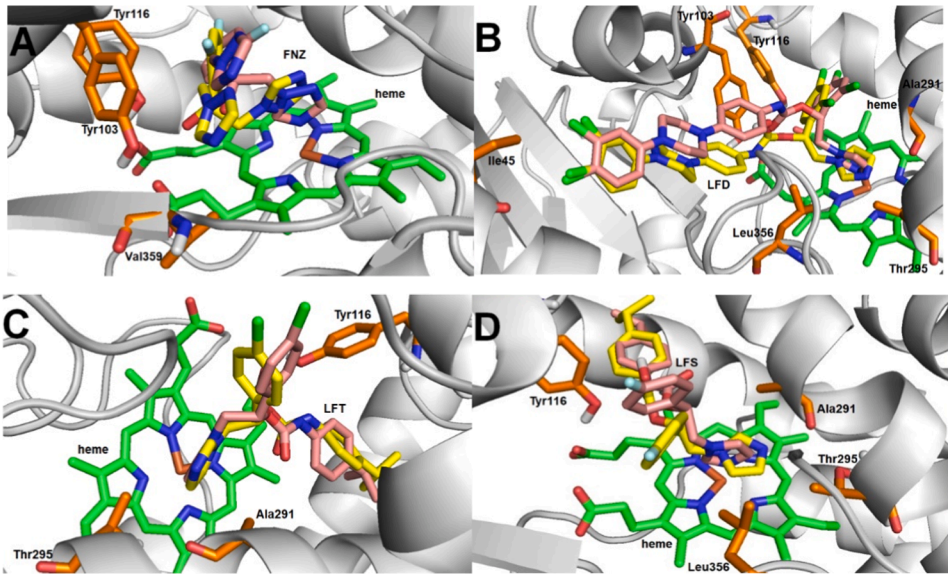

Fig. 10. Molecular Redocking of the *Trypanosoma cruzi* 14-α-Lanosterol Demethylase (CYP51) Inhibitors showing the superposition of ligands poses. (**A**) Fluconazole (FNZ) crystal conformation (magenta) and redocking pose (yellow); (**B**) Compound LFD crystal conformation (magenta) and redocking pose (yellow); (**C**) Compound LFT crystal conformation (magenta) and redocking pose (yellow); (**D**) Compound LFS crystal conformation (magenta) and redocking pose (yellow). (For interpretation of the references to color in this figure legend, the reader is referred to the web version of this article.)

Table 4
Root Mean Square Deviation (RMSD) Obtained by Molecular Redocking of the *Trypanosoma cruzi* 14-α-Lanosterol Demethylase (CYP51) Inhibitors.

PDB Code	Redocking	RMSD (Å)
2WX2	CYP51/FNZ	1.97
4CK8	CYP51/LFD	1.90
4CK9	CYP51/LFT	1.65
4CKA	CYP51/LFS	1.71

than 17**d**, respectively, 422.3 μM (Fig. 6**E**) and 247.4 μM (Fig. 6**F**). Substance **19e** obtained a CC_{50} of 259.6 μM (Fig. 6**G**). The results obtained so far indicate that the **16f** molecule is the one with the least capacity to cause toxicity, although derivatives **16d**, **16e**, **17d**, **17e**, **17f**, and **19** demonstrated low toxicity with CC_{50} values above 100 μM. These results observed for analogs **16e**, **16f**, and **17d** were higher than published by the group with ninety-two examples of 1,2,3-triazoles [30]. In this paper, the analogs **11b** and **11c** were no toxic with CC_{50} values of 0.529 mM and 0.254 mM on peritoneal macrophages, respectively (Fig. 6).

We performed treatments varying the concentrations of analogs from

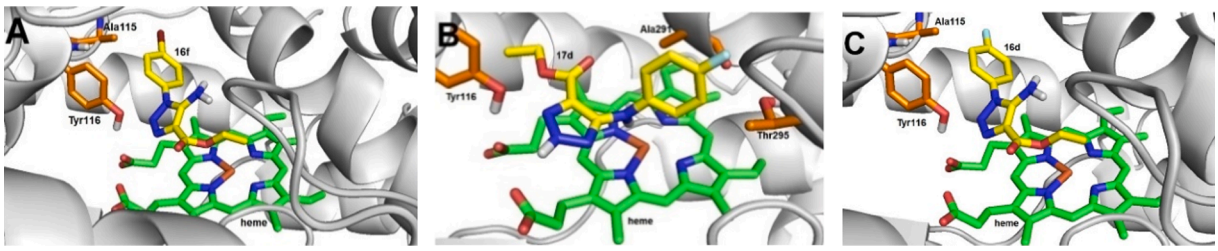

Fig. 11. Molecular Docking in 14-α-Lanosterol Demethylase (PDB code: 4CK9) of the three more active TD series compounds against *Trypanosoma cruzi*. (**A**) **16f**, (**B**) **17d** and (**C**) **16d**.

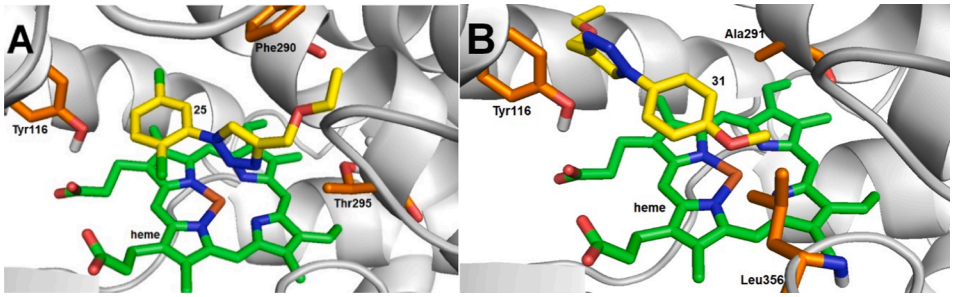

Fig. 13. Molecular Docking in 14-α-Lanosterol Demethylase (PDB code: 4CK9) of two triazole derivatives compounds active against *Trypanosoma cruzi*. (**A**) **11b** and (**B**) **11c**.

Table 5
The Heat of Formation calculated for the ligands binding to *Trypanosoma cruzi* 14-α-Lanosterol Demethylase (CYP51).

Molecular System	Heat of Formation (kcal/mol)*
CYP51/LFT	−39.30
CYP51/25	−28.36
CYP51/31	−27.00
CYP51/16f	−22.32
CYP51/17d	−18.73
CYP51/16d	−16.32

* $\Delta H_f = \Delta H_f(\text{complex}) - \Delta H_f(\text{separate})$.

10 nM to 100 μM for 72 h in epimastigotes of the Y strain of *T. cruzi*. Derivative **16d** exhibited a potent trypanocidal action with $EC_{50} = 0.59$ μM (Fig. 7**A**). Both analog **16e** (Fig. 7**B**) and **16f** (Fig. 7**C**) obtained EC_{50} values below **16d**. Substance **17d** showed an EC_{50} of 1.99 μM (Fig. 7**D**). The analogs **17e** (Fig. 7**E**) and **17f** (Fig. 8**F**) exhibited EC_{50} of 12.54 μM and 17.48 μM, respectively, both higher than **17d**. The derivative **19** obtained an EC_{50} of 73.53 μM (Fig. 7**G**). These results indicated that substance **16d** was more potent to cause a trypanocidal action. The 1,2,3-triazoles series revealed two analogs with trypanocidal activity in the nanomolar scale. The compounds **11b** and **11a** showed a respective EC_{50} value of 0.209 μM and 0.185 μM for Y strain and 0.246 μM and 0.3 μM for Dm28-C strain [30]. However, analog **11a** was extremely toxic for mammalian cells. The 1,2,3-triazoles derivative **11c** exhibited an EC_{50} value of less than 10 μM for both parasite strains with satisfactory low toxicity. The analogs **16d** and **17d** presented reducing potency against *T. cruzi* epimastigote forms when compared with **11b**. However, both 2*H*-1,2,3-triazole-4-carboxylates analogs exhibited no toxic effect on mammalian cells higher than **11b**. Interestingly, the analog **16f** and the 1,2,3-triazole **11c** showed similar potency against epimastigote Y strain. However, **16f** analog exhibited less toxic than the thirty-one compounds.

We calculated the selectivity index (SI) of the samples compared to the reference drug, benznidazole. Although the epimastigote form is infective for the intermediate host (triatominae), we use this index to indicate whether the sample has the potential to continue experiments on other forms of the parasite. We consider molecules with SI below 10 to be inappropriate for further testing. In this sense, all molecules can proceed to the assays in the trypomastigote form, except the analog **19** (Table 3). The substance with the highest SI was **16f** with a value 100 times above benznidazole. Another promising analog was **17d** with a SI 50 times higher than the reference drug. When we compared with 1,2,3-triazole analog with 2*H*-1,2,3-triazole-4-carboxylates concerning S.I. index, the compound **11b** exhibit S.I. values above to two thousand for Y strain and Dm-28c strain [30].

The selected analogs were tested in the trypomastigote form for 24 h. The derivatives **16e**, **17e,** and **17f** were not effective in reducing the viability of the parasites (Fig. 8**B, E and F**). Substances **16d** and **17d** reduced the viability of the parasites in a dose-dependent manner. The higher concentration tested showed an effect similar to benznidazole (Fig. 8**A and D**). Analog **16f** reduced the viability in the EC_{50} value obtained in epimastigotes and the concentration twice lower than the EC_{50} in a similar way to the effect of benznidazole. The highest concentration tested, twice the EC_{50} value, was more effective than benznidazole (Fig. 8**C**). However, the maximal concentration used for **16f** was ten times higher than **16d** and **17d**.

Three analogs with action on trypomastigote forms were evaluated concerning mechanism of action associated with toxic effect. The analogs **16d**, **16f**, and **17d** were tested in the concentration of 10 μM and the membrane rupture was measured for ethidium bromide entry after 24 h (Fig. 9**A**). All substances promoted plasma membrane rupture with dye entry compatible to benznidazole and the positive control with Triton X-100. This mechanism of action was similar to observed for 1,2,3-triazole analogs **11b** and **11c** on epimastigotes [30]. These substances ruptured the plasma membrane from parasites after 3 h or 24 h of treatment in Y strains and Dm-28c strain.

We investigated the binding affinities of all three compounds against CYP51 from *T. cruzi* (CYP51Tc). The sterol 14a-demethylase (CYP51) is a cytochrome P450 heme thiolate-containing enzyme involved in biosynthesis of ergosterol and ergosterol-like as major membrane components in *T. cruzi* [58-60]. CYP51 activity may be blocked by azoles resulting in cytostatic or cytotoxic consequences. Remarkably, the binding affinities of compounds **16d, 16f,** and **17d** to CYP51Tc were 4.5, 2.5, and 6.6-fold respectively higher that of the antifungal CYP51 inhibitor fluconazole, which was used as a reference (Fig. 10**B, C, and D**).

Molecular redocking was used to assess the accuracy of the docking method used to identify the poses of known inhibitors. The results indicated that the RMSD of the poses of all evaluated inhibitors are below of 2 Å (Table 4). Fig. 10 shows the poses obtained in the redocking superimposed with the conformations of the compounds present in the evaluated crystalline structures. The evaluated inhibitors were fluconazole (FNZ), LFD, LFT and LFS. All poses of these inhibitors were reproduced properly by the molecular docking approach employed.

Interestingly, the three most promising candidates are the most soluble in an aqueous solution compared to the others in the series. This factor may explain the higher activity of these prototypes, despite the similarity between their structures. When these three prototypes are compared to each other, the solubility is very similar. However, compound **16d** has higher stability after 1 h of solution preparation than **17d** and **16f**, respectively (data not shown).

The molecular docking of the three most active compounds in the 1*H*-1,2,3-triazoles series against *T. cruzi* was performed on the protein 14-α-Lanosterol Demethylase (CYP51). The results indicate that residues Ala115, Tyr116 and Thr295 appear important for the affinity of compounds **16f**, **17d** and **16d** with the molecular target. The compounds **16f** and **16d** present a similar conformational pose, however the fluorine atom present in the compound **16d** is being more favorable for hydrophobic interactions in the region close to the Ala115 residue than the bromine atom present in the compound **16f**. Both compounds appear to perform hydrogen bonds with the Tyr116 residue and with the heme group (Fig. 11). The compound **17d** presents a different pose from the compounds **16f** and **16d.** However, **17d** does intermolecular interactions in the same binding site in the CYP51 protein. Intermolecular interactions are mainly hydrogen bonds and hydrophobic interactions. The fluorine atom attached to the phenyl ring appears to play an important role in the affinity for the area formed by the Ala291 and Thr295 residues. The compound **17d** makes hydrogen bonds mainly with the Tyr116 residue and the heme group.

When compared with triazoles previously published [30], the molecular docking results of the compounds **11b** and **11c** indicate different poses. For both ligands, residue Tyr116 seems to be relevant to intermolecular interactions. The results also suggest that compound **11b** makes hydrophobic interactions to residues Phe290 and Thr295, and compound **11c** makes hydrophobic interactions to residues Ala291 and Leu356. The pose of **11b** indicates that this ligand has more probability of coordinating the amine of the triazole group to the iron atom of the heme group. In contrast, compound **11c** seems to orientate the oxygen atom of methoxyl to the heme group (Fig. 12).

The heat of formation (ΔH_f) was calculated using ligands separate and complexed to protein CYP51 in order to indicate the affinity between interacting molecules. Binding enthalpy was also obtained to a molecular system with the known inhibitor LFT. In general, all ligands studied showed favorable binding enthalpy with CYP51 (Table 5). Binding enthalpies of the ligands studied are different such as the binding modes. Compound **11b** coordinates the amine of the triazole group to the iron atom of the heme group. Compound **11c** orientates methoxyl oxygen atom to an area between the aromatic amine and iron atom of the heme group. Compounds **16f** and **16d** orientate the terminal methyl group to the aromatic area of the heme group indicating a CH/π interaction. Compound **17d** orientates the secondary amine to an area between the iron atom and aromatic amine of the heme group.

4. Conclusion

Two series of triazoles were obtained from the 1,3-dipolar cycloaddition reaction between ethyl cyanoacetate and several phenyl azides. Reaction conditions were studied to obtain 1*H*- and 2*H*-1,2,3-triazoles and unequivocal analysis of their structures. Both series were shown to be active against the epimastigote form of *T. cruzi*. The biological results indicated that molecules **16d**, **16e**, **16f**, **17d**, **17e** and **17f** are good candidates with S.I. over 10. Molecules **16e**, **17e** and **17f** are good candidates for having SI between 10 and 100. The **16d** molecule is a good candidate with an S.I. value between 100 and 200. Molecules **17d** and **16f** are excellent candidates with S.I. values above 200 times. Analog **19** showed the lowest selectivity index (below 10), so it is not a good target molecule to develop a drug with activity against the epimastigote form of *T. cruzi.* The candidates **16d**, **16f**, and **17d** showed toxic action on trypomastigotes with efficacy similar to benznidazole. The analogs **16d** and **17d** were better candidates with higher potency than **16f** in trypomastigotes. The three analogs disrupted the plasma membrane of trypomastigotes acting on CYP51 and inhibiting the ergosterol synthesis. The candidate **16d** exhibited a better profile is being more favorable to interacting with CYP51.

Declaration of Competing Interest

The authors declare that they have no known competing financial interests or personal relationships that could have appeared to influence the work reported in this paper.

Acknowledgments

The authors would like to acknowledge the agencies that funded our research: CNPq, CAPES and FAPERJ. The fellowships granted by FAPERJ (E-26/202.800/2017, E-26/010.101106/2018, E-26/010.003002/2014); CNPq 301873/2019-4, 306011/2020-4 and CAPES Financial Code 001, as well as FIOCRUZ for the HRMS analyses. The authors thank LDRX-UFF (www.ldrx.uff.br/) for the X-ray diffraction analysis and for the facilities.

Appendix A. Supplementary material

Supplementary data to this article can be found online at https://doi.org/10.1016/j.bioorg.2021.105250.

References

[1] R. Kharb, P.C. Sharma, M.S. Yar, Pharmacological significance of triazole scaffold, J. Enzyme Inhib. Med. Chem. 26 (1) (2011) 1–21, https://doi.org/10.3109/14756360903524304.
[2] K. Bozorov, J. Zhao, H.A. Aisa, 1,2,3-Triazole-containing hybrids as leads in medicinal chemistry: a recent overview, Bioorg. Med. Chem. 27 (16) (2019) 3511–3531, https://doi.org/10.1016/j.bmc.2019.07.005.
[3] W. Dehaen, V.A. Bakulev, Chemistry of 1,2,3-triazoles in Topics in Heterocyclic Chemistry, (Eds.), Springer, Switzerland, 2015.
[4] C. Therrien, R.C. Levesque, Molecular basis of antibiotic resistance and β-lactamase inhibition by mechanism-based inactivators: perspectives and future directions, FEMS Microbiol. Rev. 24 (3) (2000) 251–262, https://doi.org/10.1111/j.1574-6976.2000.tb00541.x.
[5] M. Delgado-Valverde, E. Torres, A. Valiente-Mendez, B. Almirante, S. Gómez-Zorrilla, N. Borrell, J.E. Corzo, M. Gurgui, M. Almela, L. García-Álvarez, M. C. Fontecoba-Sánchez, L. Martínez-Martínez, R. Cantón, J. Praena, M. Causse, B. Gutiérrez-Gutiérrez, J.A. Roberts, A. Farkas, Á. Pascual, J. Rodríguez-Baño, Impact of the MIC of piperacillin/tazobactam on the outcomefor patients with bacteraemia due to Enterobacteriaceae: the Bacteraemia-MIC project, J. Antimicrob. Chemother. 71 (2) (2016) 521–530, https://doi.org/10.1093/jac/dkv362.
[6] T.E. Long, J.T. Williams, Cephalosporins currently in early clinical trials for the treatment of bacterial infections, Expert Opin. Investig. Drugs 23 (10) (2014) 1375–1387, https://doi.org/10.1517/13543784.2014.930127.
[7] C.C. Blackwell, E.H. Freimer, G.C. Tuke, *In vitro* evaluation of the new oral cephalosporin cefatrizine: comparison with other cephalosporins, Antimicrob. Agents Chemother. 10 (2) (1976) 288–292, https://doi.org/10.1128/AAC.10.2.288.
[8] S. Hakimian, A. Cheng-Hakimian, G.D. Anderson, J.W. Miller, Rufinamide: a new anti-epileptic medication, Expert Opin. Pharmacother. 8 (12) (2007) 1931–1940, https://doi.org/10.1517/14656566.8.12.1931.
[9] M.J. Brodie, W.E. Rosenfeld, B. Vazquez, R. Sachdeo, C. Perdomo, A. Mann, S. Arroyo, Rufinamide for the adjunctive treatment of partial seizures in adults and adolescents: a randomized placebo-controlled trial, Epilepsia 50 (2009) 1899–1909, https://doi.org/10.1111/j.1528-1167.2009.02160.x.
[10] C. Johannessen Landmark, P.N. Patsalos, Drug interactions involving the new second- and third-generation antiepileptic drugs, Expert Rev. Neurother. 10 (1) (2010) 119–140, https://doi.org/10.1586/ern.09.136.
[11] V.F. Ferreira, D.R. da Rocha, F.C. da Silva, P.G. Ferreira, N.A. Boechat, J. L. Magalhães, Novel 1H–1,2,3-, 2H–1,2,3-, 1H–1,2,4- and 4H–1,2,4-triazole

derivatives: a patent review (2008–2011), Expert Opin. Ther. Pat. 23 (3) (2013) 319–331, https://doi.org/10.1517/13543776.2013.749862.
[12] F.C. da Silva, M.F.C. Cardoso, P.G. Ferreira, V.F. Ferreira, Biological properties of 1H-1,2,3- and 2H-1,2,3-triazole in: W. Dehaen, V.A. Bakulev (Eds.), Chemistry of 1,2,3-triazoles. Topics in Heterocyclic Chemistry, vol. 40, Springer, Cham., 2015, pp. 117–166. doi: 10.1007/7081_2014_124.
[13] R. Huisgen, 1.3-Dipolare cycloadditionen rückschau und ausblick, Angew. Chem. Int. Ed. 75 (13) (1963) 604–637, https://doi.org/10.1002/(ISSN)1521-375710.1002/ange.v75:1310.1002/ange.19630751304.
[14] R. Huisgen, Kinetics and mechanism of 1,3-dipolar cycloadditions, Angew. Chem. Int. Ed. 2 (1963) 633–645, https://doi.org/10.1002/anie.196306331.
[15] H.C. Kolb, M.G. Finn, K.B. Sharpless, Click-Chemie: diverse chemische Funktionalität mit einer Handvoll guter Reaktionen, Angew. Chem. Int. Ed. 113 (2001) 2056–2075, https://doi.org/10.1002/1521-3757(20010601)113:11%3C2056::AID-ANGE2056%3E3.0.CO;2-W.
[16] H.C. Kolb, M.G. Finn, K.B. Sharpless, Click chemistry: diverse chemical function from a few good reactions, Angew. Chem. Int. Ed. 40 (2001) 2004–2021, https://doi.org/10.1002/1521-3773(20010601)40:11%3C2004::AID-ANIE2004%3E3.0.CO;2-5.
[17] P. Wu, V.V. Fokin, Catalytic azide-alkyne cycloaddition: reactivity and applications, Aldrichim. Acta 40 (2007) 7–17, https://doi.org/10.1002/chin.200736242.
[18] C.-H. Zhou, Y. Wang, Recent researches in triazole compounds as medicinal drugs, Curr. Med. Chem. 19 (2012) 239–280, https://doi.org/10.2174/092986712803414213.
[19] H.C. Kolb, K.B. Sharpless, The growing impact of click chemistry on drug discovery, Drug Discov. Today 8 (24) (2003) 1128–1137, https://doi.org/10.1016/S1359-6446(03)02933-7.
[20] J. Wei, Y. Wang, X.L. Wang, Recent advances of 1, 2, 3-triazole compounds in medicinal chemistry, J. Chin. Pharm. Sci. 46 (2011) 481–485.
[21] L.S.M. Forezi, M.F.C. Cardoso, D.T.G. Gonzaga, F.C. da Silva, V.F. Ferreira, Alternative routes to the click method for the synthesis of 1,2,3-triazoles, an important heterocycle, Curr. Top. Med. Chem. 18 (2018) 1428–1453, https://doi.org/10.2174/1568026618666180821143902.
[22] L.S.M. Forezi, C.G.S. Lima, A.A.P. Amaral, P.G. Ferreira, M.C.B.V. de Souza, A. C. Cunha, F.C. da Silva, V.F. Ferreira, Bioactive 1,2,3-triazoles: an account on their synthesis, structural diversity and biological applications, Chem. Rec. 21 (2021), https://doi.org/10.1002/tcr.202000185. In Press.
[23] D.I. Leite, F.d.V. Fontes, M.M. Bastos, L.V.B. Hoelz, M.d.C.A.D. Bianco, A.P. de Oliveira, P.B. da Silva, C.F. da Silva, D.d.G.J. Batista, A.N.S. da Gama, R.B. Peres, J. D.F. Villar, M.d.N.C. Soeiro, N. Boechat, New 1,2,3-triazole-based analogues of benznidazole for use against Trypanosoma cruzi infection: In vitro and in vivo evaluations, Chem. Biol. Drug Des. 92 (3) (2018) 1670–1682, https://doi.org/10.1111/cbdd.13333.
[24] E.N. Silva-Jr, M.A.B.F. Moura, A.V. Pinto, M.C.F.R. Pinto, M.C.B.V. de Souza, A. J. Araújo, C. Pessoa, L.V. Costa-Lotufo, R.C. Montenegro, M.O. Moraes, V. F. Ferreira, M.O.F. Goulart, Cytotoxic, trypanocidal activities and physicochemical parameters of nor-β-lapachone-based 1,2,3-triazoles, J. Braz. Chem. Soc. 20 (2009) 635–643, https://doi.org/10.1590/S0103-50532009000400007.
[25] S. Brand, E.J. Ko, E. Viayna, S. Thompson, D. Spinks, M. Thomas, L. Sandberg, A. F. Francisco, S. Jayawardhana, V.C. Smith, C. Jansen, M. Rycker, J. Thomas, L.M. M. Osuna-Cabello, J. Riley, P. Scullion, L. Stojanovski, F.R.C. Simeons, O. Epemolu, Y. Shishikura, S.D. Crouch, T.S. Bakshi, C.J. Nixon, I.H. Reid, A.P. Hill, T. Z. Underwood, S.J. Hindley, S.A. Robinson, J.M. Kelly, J.M. Fiandor, P.G. Wyatt, M. Marco, T.J. Miles, K.D. Read, I.H. Gilbert, Discovery and Optimization of 5-Amino-1,2,3-triazole-4-carboxamide Series against Trypanosoma cruzi, J. Med. Chem. 60 (2017) 7284–7299, https://doi.org/10.1021/acs.jmedchem.7b00463.
[26] T.B. Cassamale, E.C. Costa, D.B. Carvalho, N.S. Cassemiro, C.C. Tomazela, M.C. S. Marques, M. Ojeda, M.F.C. Matos, S. Albuquerque, C.C.P. Arruda, A.C.M. Baroni, Synthesis and antitrypanosomastid activity of 1,4-diaryl-1,2,3-triazole analogues of neolignans veraguensin, grandisin and machilin G, J. Braz. Chem. Soc. 27 (2016) 1217–1228, https://doi.org/10.5935/0103-5053.20160017.
[27] B.N.M. Silva, P.A. Sales Junior, A.J. Romanha, S.M.F. Murta, C.H.S. Lima, M. G. Albuquerque, E. D'Elia, J.G.A. Rodrigues, V.F. Ferreira, F.C. Silva, A.C. Pinto, B. V. Silva, Synthesis of new thiosemicarbazones and semicarbazones containing the 1,2,3–1*H*-triazole-isatin scaffold: trypanocidal, cytotoxicity, electrochemical assays, and molecular docking, Med. Chem. 15 (3) (2019) 240–256, https://doi.org/10.2174/1573406414666180912120502.
[28] T.B. Souza, I.S. Caldas, F.R. Paula, C.C. Rodrigues, D.T. Carvalho, D.F. Dias, Synthesis, activity, and molecular modeling studies of 1,2,3-triazole derivatives from natural phenylpropanoids as new trypanocidal agents, Chem. Biol. Drug Des. 95 (2020) 124–129, https://doi.org/10.1111/cbdd.13628C.
[29] E.O.J. Porta, S.N. Jäger, I. Nocito, G.I. Lepesheva, E.C. Serra, B.L. Tekwani, G. R. Labadie, Antitrypanosomal and antileishmanial activity of prenyl-1,2,3-triazoles, MedChemComm 8 (5) (2017) 1015–1021, https://doi.org/10.1039/C7MD00008A.
[30] R.X. Faria, D.T.G. Gonzaga, P.A.F. Pacheco, A.L.A. Souza, V.F. Ferreira, F.d.C. da Silva, Searching for new drugs for Chagas diseases: triazole analogs display high in vitro activity against *Trypanosoma cruzi* and low toxicity toward mammalian cells, J. Bioenerg. Biomembr. 50 (2) (2018) 81–91, https://doi.org/10.1007/s10863-018-9746-z.
[31] O. Dimroth, Ueber intramolekulare Umlagerungen. Umlagerungen in der Reihe des 1, 2, 3-Triazols. Justus Liebigs Ann. Chem. 364 (1909) 183–226. doi: 10.1002/jlac.19093640204un.
[32] O. Dimroth, W. Michaelis, Intramolekulare Umlagerung der 5-Amino-1,2,3-triazole, Justus Liebigs Ann. Chem. 459 (1) (1927) 39–46, https://doi.org/10.1002/(ISSN)1099-069010.1002/jlac.v459:110.1002/jlac.19274590104.
[33] V.F. Ferreira, T.B. Silva, F.P. Pauli, P.G. Ferreira, L.S.M. Forezi, C.G.S. Lima, F.C. da Silva, Dimroths rearrangement as a synthetic strategy towards new heterocyclic compounds, Curr. Org. Chem. 24 (2020) 1999–2018, https://doi.org/10.2174/1385272824999200805114837.
[34] E. Lieber, T.S. Chao, C.N.R. Rao, Synthesis and isomerization of substituted 5-amino-l,2,3-triazoles, J. Org. Chem. 22 (1957) 654–662, https://doi.org/10.1021/jo01357a018.
[35] G.M. Sheldrick, SHELXT–Integrated space-group and crystal-structure determination, Acta Crystallogr. A C 71 (2015) 3–8, https://doi.org/10.1107/s2053273314026370.
[36] O.V. Dolomanov, L.J. Bourhis, R.J. Gildea, J.A.K. Howard, H. Puschmann, OLEX 2: a complete structure solution, refinement and analysis program, J. Appl. Cryst. 42 (2) (2009) 339–341, https://doi.org/10.1107/S0021889808042726.
[37] Z.-P. Cao, B. Quan, H.-S. Dong, Synthesis of (3,5-aryl/methyl-1*H*-pyrazol-1-yl)-(5-arylamino-2*H*-1,2,3-triazol-4-yl)methanone, J. Chin. Chem. Soc. 55 (4) (2008) 761–767, https://doi.org/10.1002/jccs.v55.410.1002/jccs.200800114.
[38] H. Wamhoff, W. Wambach, Heterocyclic β-enamino esters 51. Carbon-13 NMR studies of the Dimroth rearrangement of 1,2,3-triazoles, Chemiker Zeitung 113 (1989) 11–15.
[39] B. Wang, H.-S. Dong, The synthesis and Crystal Structure of 5-(4-bromophenylamino)-2-methylsulfanyl-2H-1,2,3-triazol-4-carboxylic acid Ethyl Ester, J. Chem. Crystalogr. 39 (2009) 95–98, https://doi.org/10.1007/s10870-008-9425-8.
[40] C. Chen, P.S. Doyle, L.V. Yermalitskaya, Z.B. Mackey, K.K.H. Ang, J.H. McKerrow, L.M. Podust, *Trypanosoma cruzi* CYP51 inhibitor derived from a mycobacterium tuberculosis screen hit, PLoS Negl. Trop. Dis. 3 (2009) e372, https://doi.org/10.1371/journal.pntd.0000372.
[41] M.D. Hanwell, D.E. Curtis, D.C. Lonie, T. Vandermeersch, E. Zurek, G.R. Hutchison, Avogadro: an advanced semantic chemical editor, visualization and analysis platform, J. Cheminf. 4 (2012) 17, https://doi.org/10.1186/1758-2946-4-17.
[42] T.A. Halgren, Merck molecular force field. I. Basis, form, scope, parameterization, and performance of MMFF94, J. Comp. Chem. 17 (1996) 490–519, https://doi.org/10.1002/(sici)1096-987x(199604)17:5/6%3C490::aid-jcc1%3E3.0.co;2-p.
[43] J.J.P. Stewart, Optimization of parameters for semiempirical methods V: Modification of NDDO approximations and application to 70 elements, J. Mol. Model. 13 (12) (2007) 1173–1213, https://doi.org/10.1007/s00894-007-0233-4.
[44] MOPAC2016, James J. P. Stewart, Stewart Computational Chemistry, Colorado Springs, CO, USA, HTTP://OpenMOPAC.net (2016).
[45] R. Thomsen, M.H. Christensen, MolDock: a new technique for high-accuracy molecular docking, J. Med. Chem. 49 (2006) 3315–3321, https://doi.org/10.1021/jm051197e.
[46] X. Du, Y. Li, Y.-L. Xia, S.-M. Ai, J. Liang, P. Sang, X.-L. Ji, S.-Q. Liu, Insights into protein-ligand interactions: mechanisms, models, and methods, Int. J. Mol. Sci. 17 (2016) 144, https://doi.org/10.3390/ijms17020144.
[47] A. Klamt, G. Schüümann, COSMO, a new approach to dielectric screening in solvents with explicit expressions for the screening energy and its gradient, J. Chem. Soc., Perkin Trans. 2 (1993) 799–805, https://doi.org/10.1039/P29930000799.
[48] James J.P. Stewart, Optimization of parameters for semiempirical methods VI: more modifications to the NDDO approximations and re-optimization of parameters, J. Mol. Model. 19 (1) (2013) 1–32, https://doi.org/10.1007/s00894-012-1667-x.
[49] N. Boechat, V.F. Ferreira, S.B. Ferreira, M.L.G. Ferreira, F.C. da Silva, M.M. Bastos, M.S. Costa, M.C.S. Lourenço, A.C. Pinto, A.U. Krettli, A.C. Aguiar, B.M. Teixeira, N. V. da Silva, P.R.C. Martins, F.A.F.M. Bezerra, A.L.S. Camilo, G.P. da Silva, C.C.P. Costa, Novel 1,2,3-Triazole Derivatives for Use against Mycobacterium tuberculosis H37Rv (ATCC 27294) Strain. J. Med. Chem. 54 (2011) 5988–5999. Doi: 10.1021/jm2003624.
[50] D.T.G. Gonzaga, L.B.G. Ferreira, T.E.M.M. Costa, N.L. von Ranke, P.A.F. Pacheco, A.P.S. Simões, J.C. Arruda, L.P. Dantas, H.R. de Freitas, R.A.M. Reis, C. Penido, M. L. Bello, H.C. Castro, C.R. Rodrigues, V.F. Ferreira, R.X. Faria, F.C. da Silva, 1-Aryl-1H- and 2-aryl-2H-1,2,3-triazole derivatives blockade P2X7 receptor *in vitro* and inflammatory response *in vivo*, Eur. J. Med. Chem. 139 (2017) 698–717, https://doi.org/10.1016/j.ejmech.2017.08.034.
[51] B.R. Brown, D.L. Hammick, S.G. Heritage, 781. The Tautomerism of 5-Amino-1-aryl-l:2:3-triazoles, J. Chem. Soc. (1953) 3820–3825, https://doi.org/10.1039/JR9530003820.
[52] A. Dornow, J. Helberg, Synthesis of nitrogen-containing heterocycles, XXIV. Preparation and ortho-condensation of some 4,5-disubstituted 1,2,3-triazoles, Chem. Ber. 93 (1960) 2001–2010, https://doi.org/10.1002/cber.19600930914.
[53] E. Lieber, T.S. Chao, C.N.R. Rao, Synthesis and isomerization of substituted 5-amino-1,2,3-triazoles, J. Org. Chem. 22 (1957) 654–662, https://doi.org/10.1021/jo01357a018.
[54] H. Wamhoff, J. Bohlen, S.Y. Yangt, Heterocyclic β-enamino esters 43 - Easy "C NMR distinction between aryl-substituted dimroth isomers of the 1,2,3-triazole series, Magn. Reson. Chem. 24 (1986) 809–811, https://doi.org/10.1002/mrc.1260240914.
[55] N.R. Ayyangar, K.V. Srinivasan, Effect of substituents in the for mation of diacetanilides, Can. J. Chem. 62 (1984) 1292–1296.
[56] R. Goddard, O. Heinemann, C. Krüger, Pyrrole and a Co-crystal of 1H- and 2H–1,2,3-Triazole, Acta Crystallogr. C 53 (1997) 1846–1850, https://doi.org/10.1107/S0108270197009682.

[57] J.-L.M. Abboud, C. Foces-Foces, R. Notario, R.E. Trifonov, A.P. Volovodenko, V. A. Ostrovskii, I. Alkorta, J. Elguero, Basicity of N-H- and N-methyl-1,2,3-triazoles in the gas phase, in solution, and in the solid state – an experimental and theoretical study, Eur. J. Org. Chem. (2001) 3013–3024, https://doi.org/10.1002/1099-0690(200108)2001:16%3C3013::AID-EJOC3013%3E3.0.CO;2-Y.

[58] Y. Aoyama, Recent progress in the CYP51 research focusing on its unique evolutionary and functional characteristics as a diversozyme P450, Front. Biosci. 10 (2005) 1546–1557, https://doi.org/10.2741/1639.

[59] Stephen T. Furlong, Sterols of parasitic protozoa and helminths, Exp. Parasitol. 68 (4) (1989) 482–485, https://doi.org/10.1016/0014-4894(89)90134-3.

[60] C.W. Roberts, R. McLeod, D.W. Rice, M. Ginger, M.L. Chance, L.J. Goad, Fatty acid and sterol metabolism: potential antimicrobial targets in apicomplexan and trypanosomatid parasitic protozoa, Mol. Biochem. Parasitol. 126 (2) (2003) 129–142, https://doi.org/10.1016/S0166-6851(02)00280-3.